

Higher twist corrections to doubly-charmed baryonic B decays

Zhou Rui,^{*} Zhi-Tian Zou,[†] and Ying Li[‡]

Department of Physics, Yantai University, Yantai 264005, China
(Dated: December 31, 2024)

Baryonic two-body B mesons decays have been measured experimentally for some time, which provides an excellent ground for studying the QCD of baryonic B decays. In this work, we investigate the two-body doubly-charmed baryonic B decays in the perturbative QCD (PQCD) approach including higher twist contributions to the light-cone distribution amplitudes (LCDAs). The charmed baryon LCDAs are included up to the twist four and the effect of the subleading component of the B meson LCDAs is studied for details. With the inclusion of these higher-power contributions, the PQCD results on rates can explain the current experimental data well. Moreover, we note that the SU(3) symmetry breaking is important in the concerned processes and play an essential role in understanding the measurements of $\mathcal{B}(\bar{B}^0 \rightarrow \Lambda_c^+ \bar{\Lambda}_c^-)$ and $\mathcal{B}(B^- \rightarrow \Xi_c^0 \bar{\Lambda}_c^-)$. We also evaluate the angular asymmetries for the first time, which have neither been measured experimentally nor calculated theoretically. All these predictions can be tested in future.

PACS numbers: 13.25.Hw, 12.38.Bx, 14.40.Nd

I. INTRODUCTION

It is well known that exclusive B -decays offer an excellent laboratory for testing factorization, uncovering the nature of the QCD dynamics, revealing potential signals of CP violation, and searching for the effects of the new physics beyond the Standard Model (SM). Compared with the mesonic B -decays, the exclusive baryonic decays of B mesons have many unique signatures due to the half integral spins of the final state baryons, which provides fruitful physical observables in experiments. Theoretical studies of the baryonic B decays are important for the understanding of the whole the B -physics sector. Particularly, the B factories and LHCb experiments have found some new phenomenons, such as the threshold enhancement [1, 2], hierarchy of branching fractions for multi-body modes [3], and angular correlation puzzle [4-7], which pose a great challenge to theorists.

In the SM, baryons can be produced only as baryon-antibaryon pairs due to the conservation of the baryon-number. Many light mesons decay to baryon pair are forbidden because of the insufficient phase space. However, B meson is heavy enough to allow a baryon-antibaryon pair or even doubly charmed baryon pair production in the final state, providing a unique setting for shedding light on the baryon-production mechanisms. The experimental measurements for baryonic B decays have a long history, including the asymmetric e^+e^- collider experiments BaBar and Belle [8] and the pp collision LHCb [9, 10]. Reviews of the experimental and theoretical status of exclusive baryonic B decays could be referred to Refs [11, 12]. However, the theoretical description of non-leptonic two-body B decays is notoriously complicated.

The dynamics of baryonic B decay is complex and poorly understood theoretically. One of the common and conspicuous features for baryonic B decay is the threshold enhancement [13]. As conjectured in Ref. [14], the dibaryon mass spectra shows a strong enhancement near the threshold, the decay rates of two-body baryon-antibaryon final states are suppressed relative to rates of multi-body final states containing the same baryon-antibaryon pair. In this configuration the baryon-antibaryon pair prefers to be produced collinearly rather than back-to-back in baryonic B decays [6, 7, 14]. Moreover, Belle Collaboration [15, 16] also observe the hierarchy of branching ratios for two-body modes: the decays to two charmed baryons have rates larger than the single charmed baryonic processes and the latter have larger branching ratios than the charmless decays. For example, the measured branching ratios have the pattern [17]

$$\mathcal{B}(B^- \rightarrow \bar{\Lambda}_c^- \Xi_c^0) (\sim 10^{-3}) \gg \mathcal{B}(\bar{B}^0 \rightarrow \bar{p} \Lambda_c^+) (\sim 10^{-5}) \gg \mathcal{B}(\bar{B}^0 \rightarrow \bar{p} p) (\sim 10^{-8}), \quad (1)$$

*Electronic address: jindui1127@126.com

†Electronic address: zouzt@ytu.edu.cn

‡Electronic address: liying@ytu.edu.cn

for two-body baryonic B decays. Note that the Cabibbo-Kobayashi-Maskawa (CKM) matrix element and the phase space factor does not lead to such a clear hierarchy of branching ratios, there must be a certain mechanism to enhance or suppress specific processes. Earlier calculations based on QCD sum rules [18] or the diquark model [19] predict that the single charmed baryonic B decays are comparable with the double ones, shows great tension with the experiments. Phenomenologically, the preference could also be qualitatively comprehended in terms of the threshold enhancement as a charmed baryon is heavier than a light baryon and the thresholds for baryon pair with more charmed baryons are closer to the B meson mass. There have been several work describe the threshold peaking behavior based on the Gluonic and fragmentation mechanisms [13], Pole models [6], and Intermediate $X(1835)$ baryonium bound state [20]. However, how to quantitatively evaluate their absolute decay rates and how to understand their distinct dynamics deserve more detailed studies, especially for the QCD-inspired approaches.

In this work, we attempt to provide some quantitative insights into their dynamics, and concentrate primarily on the two-body doubly charmed baryonic B decays, which have attracted both experimental and theoretical attention. In the past few years, the LHCb and Belle collaborations had published the observations of $B^- \rightarrow \bar{\Lambda}_c^- \Xi_c^0$ [21], $\bar{B}^0 \rightarrow \bar{\Lambda}_c^- \Xi_c^+$ [22], and $\bar{B}_{(s)}^0 \rightarrow \Lambda_c^+ \bar{\Lambda}_c^-$ [23], with the branching ratios ranging from 10^{-6} to 10^{-3} . Also, some final states involving excited Ξ_c states, such as $B^- \rightarrow \bar{\Lambda}_c^- (\Xi_c^{\prime 0}, \Xi_c^0(2645, 2790))$, were observed by Belle [24], which provide an experimental research platform to investigate the Ξ_c excitation spectrum in the baryonic B decays. These experimental results on B meson baryonic decays are of a great importance to advance the understanding of the QCD. The key is to understand quantitatively the decay mechanism of the two-body decays. Some theoretical predictions for their branching fraction are available. In Refs. [25, 26], the authors assume that $\bar{B} \rightarrow \Xi_c \bar{\Lambda}_c$ is produced from a soft $q\bar{q}$ quark pair through the π and σ meson exchanges rather than the hard gluon exchanges, the predicted branching ratios are at the level of 10^{-3} . This magnitude is also supported by the estimation from final state interactions (FSIs) [27]. Very recently, two-body doubly charmed baryonic decays were investigated within the framework of SU(3) flavor symmetry [28]. With the determination of the SU(3) flavour parameters, they have predicted the branching ratios, which can be well approximated agrees with the experimental data. These efforts may allow a better understanding of the threshold enhancement, and explain the hierarchy trend of the branching fractions for baryonic B decays.

As the PQCD has achieved a preliminary success in the mesonic B decays [29–34] and Λ_b baryon decays [35–48], it is natural to extend this approach to evaluate the decay rates of baryonic decays of B mesons, and the first attempt to calculate the $\bar{B}^0 \rightarrow \bar{p} \Lambda_c^+$ decay has been performed in [49]. Our emphasis in this work is to establish PQCD formalism for the two-body doubly charmed baryonic B decays. Although the energy release in the concerned channels is small due to the two heavy charmed baryons in the final states, similar processes such as decays of B mesons to two charmed mesons have been well studied in the PQCD approach [50, 51], with the best agreement with experiments. We still assume that these processes are dominated by hard gluon exchanges. In this case, it is believed that some higher-power corrections may be numerically important. Here we will analyze these processes by including the subleading B meson LCDAs and charmed baryon LCDAs up to twist 4 level. It will be shown that the inclusion of these higher-twist contributions improves the agreement of our results with data. Aside from the decay branching ratio, many asymmetry parameters are also predicted for the first time, which could be checked by future experiments.

The layout of this paper is as following. After presenting the effective hamiltonian, kinematics, and the light-cone distribution amplitudes (LCDAs) of the initial and final states in Sec. II, we give a general PQCD formalism for the two-body doubly charmed baryonic B decays. The numerical results for the invariant amplitudes, decay branching ratios, and various asymmetries are presented in Sec. III. Finally, Sec. IV will be the conclusion of this work. Some details of the factorization formulas are displayed in Appendix A.

II. THEORETICAL FRAMEWORK

The topology of the two-body baryonic B -meson decay is similar to that of the two-body baryon decay because they both involve two baryons and one meson in the initial and final states. In this case, the PQCD calculations of the two-body baryonic B -meson decay also start at the order of $\mathcal{O}(\alpha_s^2)$, which requires at least two hard gluon exchanges in the leading order approximation. The quark diagrams for $B^- \rightarrow \Xi_c^0 \bar{\Lambda}_c^-$ mode involve the internal W -emission diagrams for $b \rightarrow c$ (the first two rows in Fig. 1), the penguin loop diagrams for $b \rightarrow s$ transition (the first topology in the last row), and the weak annihilation diagrams for $b \rightarrow u$ (the last topology). Contributions from the penguin loop diagrams and the weak annihilation diagrams suffer highly loop suppressed and CKM suppression, respectively, compared with the Cabibbo-favored $b \rightarrow c$ W -emission diagrams. Moreover, in both the penguin and weak annihilation diagrams, a back-to-back $c\bar{c}$ pair is created by a hard gluon, which is far off the mass shell. It should be harder than that produces a light quark pair in the W -emission diagrams, resulting in an additional dynamical suppression to the penguin and weak annihilation diagrams. An explicit evaluation shows that the contributions from the penguin and weak annihilation topologies can be safely neglected in the following analyses.

The $\bar{B}^0 \rightarrow \Xi_c^+ \bar{\Lambda}_c^-$ mode shares an isospin relation with $B^- \rightarrow \Xi_c^0 \bar{\Lambda}_c^-$, we do not repeat the corresponding diagrams

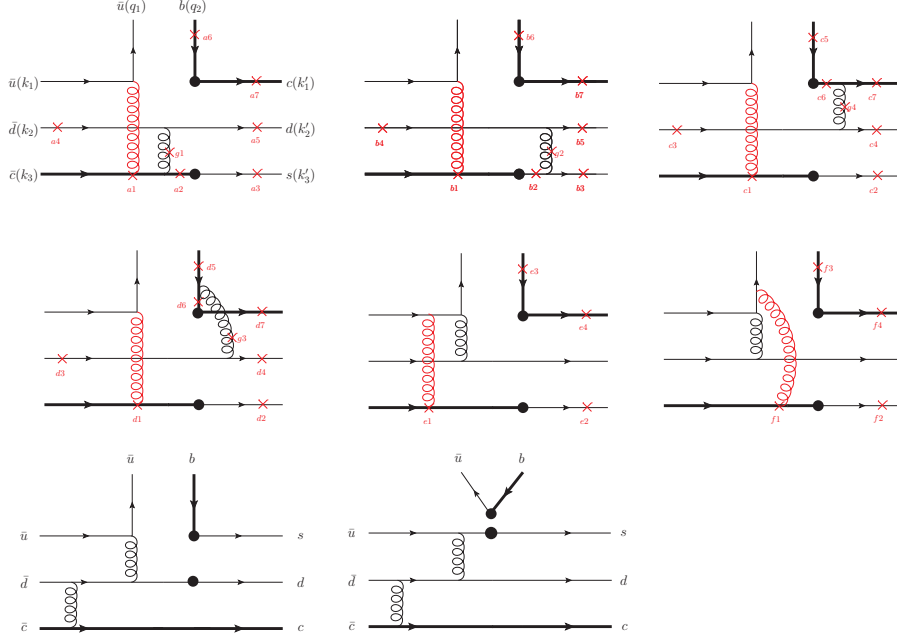


FIG. 1: Topological diagrams contributing to the $B^- \rightarrow \Xi_c^0 \bar{\Lambda}_c^-$ decay, where the solid black blob represents the vertex of the effective weak interaction. The heavy quarks b and c are shown in bold lines. The crosses indicate the possible connections of the gluon (red) attached to the spectator \bar{u} quark. The first two rows are classified as the W -emission diagrams, while the last two topologies denote the penguin and weak annihilation diagrams, respectively. Here, we only draw one representative Feynman diagram for each of the last two topologies.

here. The decay of $\bar{B}_s^0 \rightarrow \Lambda_c^+ \bar{\Lambda}_c^-$ is fed by the W -exchange and penguin-annihilation topologies as shown in Fig. 2. The first two rows are the dominant W -exchange diagrams induced by $b \rightarrow c$. In the last row, the first topology is another W -exchange diagram induced by $b \rightarrow u$ and the last one is the penguin-annihilation diagram induced by $b \rightarrow s$. Their contributions suffer from severe suppression as the same reason aforementioned. $\bar{B}^0 \rightarrow \Lambda_c^+ \bar{\Lambda}_c^-$ proceeds through both the topological W -emission and W -exchange diagrams, whose diagrams can be obtained from Figs. 1 and 2 with a suitable replacement of some quark flavors thus are not explicitly given here. All these topologies can be evaluated systematically in PQCD.

The kinematic variables of the initial and final state can be defined as follows. p and p' denote the momenta of the antibaryon and baryon in the final state, respectively. $q = p + p'$ denote the momentum of the B meson. In the B rest frame, the two final-state antibaryon and baryon move back to back with large momenta. The B meson momentum in the light-cone coordinates is written as $q = \frac{M}{\sqrt{2}}(1, 1, \mathbf{0}_T)$ with M being the B meson mass. We further assume that the antibaryon (baryon) is mainly along the plus (minus) direction and write

$$p = \frac{M}{\sqrt{2}}(f^+, f^-, \mathbf{0}_T), \quad p' = \frac{M}{\sqrt{2}}(1 - f^+, 1 - f^-, \mathbf{0}_T). \quad (2)$$

The on-shell conditions of the baryon and antibaryon lead to

$$f^\pm = \frac{1}{2} \left(1 - r^2 + \bar{r}^2 \pm \sqrt{(1 - r^2 + \bar{r}^2)^2 - 4\bar{r}^2} \right), \quad (3)$$

where the mass ratio $r(\bar{r}) = m(\bar{m})/M$ with $m(\bar{m})$ being the mass of (anti)baryon. The valence quark momenta inside the initial and final state hadrons, as shown in Fig. 1, are parametrized as

$$\begin{aligned} q_1 &= \left(0, \frac{M}{\sqrt{2}}y, \mathbf{q}_T \right), & q_2 &= q - q_1, \\ k_1 &= \left(\frac{M}{\sqrt{2}}f^+x_1, 0, \mathbf{k}_{1T} \right), & k_2 &= \left(\frac{M}{\sqrt{2}}f^+x_2, 0, \mathbf{k}_{2T} \right), & k_3 &= p - k_1 - k_2, \end{aligned}$$

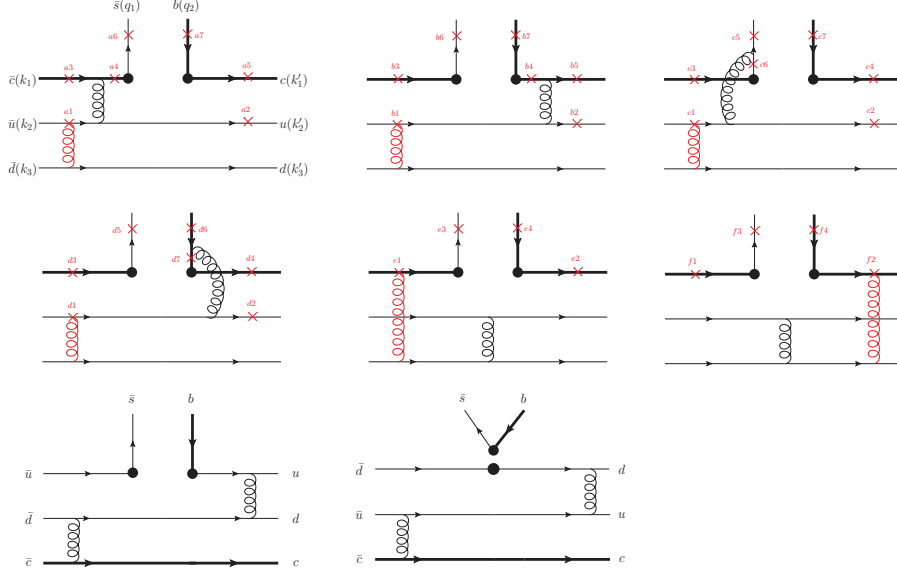


FIG. 2: Topological diagrams contributing to the $\bar{B}_s^0 \rightarrow \Lambda_c^+ \bar{\Lambda}_c^-$ decay.

$$k'_1 = p' - k'_1 - k'_2, \quad k'_2 = \left(0, \frac{M}{\sqrt{2}}(1 - f^-)x'_2, \mathbf{k}'_{2T}\right), \quad k'_3 = \left(0, \frac{M}{\sqrt{2}}(1 - f^-)x'_3, \mathbf{k}'_{3T}\right), \quad (4)$$

where q_1 is the spectator momentum on the B meson side. y and \mathbf{q}_T represent its longitudinal momentum fraction and transverse momentum, respectively. Here, the bottom and charm quarks are considered to be massive, while other light quarks are massless. All the valence quarks carry transverse momenta $\mathbf{k}_{lT}^{(l)}$ with $l = 1, 2, 3$ to smear the end-point singularities. The parton longitudinal momentum fractions $x_l^{(l)}$ vary in the range of 0 to 1. For the W -exchange diagrams in Fig. 2, the parametrization of the kinematic variables in Eq. (4) still apply except for k_1 and k_3 since in this case k_1 represents the anticharm quark momentum instead of k_3 . The new parametrization is chosen as $k_3 = \left(\frac{M}{\sqrt{2}}f^+x_3, 0, \mathbf{k}_{3T}\right)$ and $k_1 = p - k_2 - k_3$.

In the course of the PQCD calculations, the necessary inputs contain the hadronic LCDAs of the initial and final states, which can be constructed via the nonlocal matrix elements. We next specify the relevant LCDAs for the present study. After the complete classification of three-quark LCDAs of the Λ_b baryon in the heavy quark limit has been constructed [52], the investigation of Λ_b the heavy-baryon distribution amplitudes has made great progress in the last decade [52–57]. However, the LCDAs of charmed baryons have received less attention in the literature. Based on heavy-quark symmetry, we can use the same LCDAs for the baryon containing the charm quark and the bottom quark. Up to twist-4, the matrix element for the antitriplet of singly charmed baryons can be expressed in terms of the four LCDAs in the following way [57, 58]:

$$\begin{aligned} \epsilon^{ijk} \langle 0 | q_{1\alpha}^i(t_1) q_{2\beta}^j(t_2) c_\gamma^k(0) | \mathcal{B}_c \rangle &= \frac{f^{(1)}}{8} \left[(\not{n} \gamma_5 C)_{\alpha\beta} \phi_2(t_1, t_2) + (\not{n} \gamma_5 C)_{\alpha\beta} \phi_4(t_1, t_2) \right] u_\gamma \\ &+ \frac{f^{(2)}}{4} \left[(\gamma_5 C)_{\alpha\beta} \phi_3^s(t_1, t_2) - \frac{i}{2} (\sigma_{\bar{n}n} \gamma_5 C)_{\alpha\beta} \phi_3^a(t_1, t_2) \right] u_\gamma \end{aligned} \quad (5)$$

where i, j , and k are color indices, and ϵ^{ijk} is the totally antisymmetric tensor. α, β, γ are the Dirac indices and C is the charge conjugation matrix defined in terms of the Dirac matrices. u denotes the on-shell Dirac spinor for the antitriplet \mathcal{B}_c . n and \bar{n} are two light-cone vectors satisfy $n^2 = \bar{n}^2 = 0$ and $n \cdot \bar{n} = 2$. For the decay constants $f^{(1,2)}$, we use the values $f_{\Lambda_c}^{(1,2)} = 0.022 \pm 0.008 \text{ GeV}^3$ and $f_{\Xi_c}^{(1,2)} = 0.027 \pm 0.008 \text{ GeV}^3$ from the QCD sum rules [59]. $\phi_{2,3,4}$ correspond twist-2, twist-3, and twist-4 LCDAs, respectively. In the limit of the exact SU(3) flavour symmetry, they have definite symmetry properties: ϕ_3^a is antisymmetric under the exchange $t_1 \leftrightarrow t_2$, while others are symmetric. The

TABLE I: Values of the parameters ε_n (GeV), η_n (GeV), a_n , and b_n appearing in the charmed baryon LCDAs.

Baryon	ε_0	ε_1	ε_2	a_1	a_2	
Λ_c	ϕ_2	$0.201^{+0.143}_{-0.059}$	0	$0.551^{+\infty}_{-0.356}$	0	$0.391^{+0.279}_{-0.279}$
	ϕ_3^s	$0.232^{+0.047}_{-0.056}$	0	$0.055^{+0.010}_{-0.020}$	0	$-0.161^{+0.108}_{-0.207}$
	ϕ_4	$0.352^{+0.067}_{-0.083}$	0	$0.262^{+0.116}_{-0.132}$	0	$-0.541^{+0.173}_{-0.090}$
Ξ_c	ϕ_2	$0.228^{+0.068}_{-0.061}$	$0.429^{+0.654}_{-0.281}$	$0.449^{+\infty}_{-0.473}$	$0.057^{+0.055}_{-0.034}$	$0.449^{+0.236}_{-0.380}$
	ϕ_3^s	$0.258^{+0.031}_{-0.038}$	$0.750^{+0.308}_{-0.093}$	$0.520^{+0.229}_{-0.060}$	$0.339^{+0.261}_{-0.160}$	$5.244^{+0.696}_{-1.132}$
	ϕ_4	$0.378^{+0.065}_{-0.080}$	$2.291^{+\infty}_{-0.842}$	$0.286^{+0.130}_{-0.150}$	$0.039^{+0.030}_{-0.018}$	$-0.090^{+0.037}_{-0.021}$
	η_1	η_2	η_3	b_2	b_3	
Λ_c	ϕ_3^a	$0.324^{+0.054}_{-0.026}$	0	$0.633^{+0.077}_{-0.027}$	0	$-0.240^{+0.240}_{-0.147}$
Ξ_c	ϕ_3^a	$0.218^{+0.043}_{-0.047}$	$0.877^{+0.820}_{-0.152}$	$0.049^{+0.005}_{-0.012}$	$0.037^{+0.032}_{-0.019}$	$-0.027^{+0.016}_{-0.027}$

corresponding model functions in the momentum space can be written as in the Gegenbauer expansion [43, 53]

$$\begin{aligned}
\phi_2(x_2, x_3) &= x_2 x_3 m^4 \sum_{n=0}^2 \frac{a_n}{\varepsilon_n^4} C_n^{3/2} \left(\frac{x_2 - x_3}{x_2 + x_3} \right) e^{-\frac{(x_2+x_3)m}{\varepsilon_n}}, \\
\phi_3^s(x_2, x_3) &= (x_2 + x_3) m^3 \sum_{n=0}^2 \frac{a_n}{\varepsilon_n^3} C_n^{1/2} \left(\frac{x_2 - x_3}{x_2 + x_3} \right) e^{-\frac{(x_2+x_3)m}{\varepsilon_n}}, \\
\phi_3^a(x_2, x_3) &= (x_2 + x_3) m^3 \sum_{n=1}^3 \frac{b_n}{\eta_n^3} C_n^{1/2} \left(\frac{x_2 - x_3}{x_2 + x_3} \right) e^{-\frac{(x_2+x_3)m}{\eta_n}}, \\
\phi_4(x_2, x_3) &= m^2 \sum_{n=0}^2 \frac{a_n}{\varepsilon_n^2} C_n^{1/2} \left(\frac{x_2 - x_3}{x_2 + x_3} \right) e^{-\frac{(x_2+x_3)m}{\varepsilon_n}}, \tag{6}
\end{aligned}$$

with the Gegenbauer polynomials

$$C_0^\xi(x) = 1, \quad C_1^\xi(x) = 2\xi x, \quad C_2^\xi(x) = 2\xi(1 + \xi)x^2 - \xi. \tag{7}$$

Note that the parameters ε_n , η_n , a_n , and b_n in Eq. (6) differ with distinct twists. Their values evaluated at $\mu = 1$ GeV have been determined in [53], which are collected in Table I for completeness. The lowest-order Gegenbauer moments are set to 1 to comply with the normalizations [53]. We emphasize that though we employed the same forms and parameters as the bottom baryon LCDAs, but the mass m in Eq. (6) actually represents the charmed baryon mass. This results in the charmed baryon LCDAs behave differently, with exponentials decreasing more slowly in the large $x_{2,3}$ region than those in the bottom baryon LCDAs.

For the baryonic B decays, we need two projectors for an outgoing baryon and an outgoing antibaryon. The former can be derived by

$$\begin{aligned}
\epsilon^{ijk} \langle \mathcal{B}_c | \bar{q}_{1\alpha}^i(t_1) \bar{q}_{2\beta}^j(t_2) \bar{c}_\gamma^k(0) | 0 \rangle &= -\gamma_{\alpha\alpha'}^0 \gamma_{\beta\beta'}^0 \gamma_{\gamma\gamma'}^0 \epsilon^{ijk} \langle 0 | q_{1\alpha'}^i(t_1) q_{2\beta'}^j(t_2) c_{\gamma'}^k(0) | \mathcal{B}_c \rangle^\dagger \\
&= \frac{f^{(1)}}{8} \bar{u}_\gamma [(C\gamma_5 \not{\eta})_{\beta\alpha} \phi_2(t_1, t_2) + (C\gamma_5 \not{\eta})_{\beta\alpha} \phi_4(t_1, t_2)] \\
&\quad + \frac{f^{(2)}}{4} \bar{u}_\gamma [(C\gamma_5)_{\beta\alpha} \phi_3^s(t_1, t_2) + \frac{i}{2} (C\gamma_5 \sigma_{\bar{n}n})_{\beta\alpha} \phi_3^a(t_1, t_2)]. \tag{8}
\end{aligned}$$

Further perform the charge conjugation transform, we get the expression for the outgoing antibaryon

$$\begin{aligned}
\epsilon^{ijk} \langle \bar{\mathcal{B}}_c | q_{1\alpha}^i(t_1) q_{2\beta}^j(t_2) c_\gamma^k(0) | 0 \rangle &= -C_{\alpha'\alpha} C_{\beta\beta'} C_{\gamma\gamma'} \epsilon^{ijk} \langle \mathcal{B}_c | \bar{q}_{1\alpha'}^i(t_1) \bar{q}_{2\beta'}^j(t_2) \bar{c}_{\gamma'}^k(0) | 0 \rangle \\
&= -\frac{f^{(1)}}{8} v_\gamma [(\not{\eta}\gamma_5 C)_{\beta\alpha} \phi_2(t_1, t_2) + (\not{\eta}\gamma_5 C)_{\beta\alpha} \phi_4(t_1, t_2)] \\
&\quad + \frac{f^{(2)}}{4} v_\gamma [(\gamma_5 C)_{\beta\alpha} \phi_3^s(t_1, t_2) + \frac{i}{2} (\sigma_{\bar{n}n} \gamma_5 C)_{\beta\alpha} \phi_3^a(t_1, t_2)]. \tag{9}
\end{aligned}$$

where $v = C\bar{u}^T$ denote the spinor of an antiparticle.

As a heavy-light system, the B -meson distribution amplitude in fact consists of two components [60, 61]

$$\Phi_B = \frac{i}{\sqrt{2N_c}}(\not{q} + M)\gamma_5 \left(\frac{\not{n}_+}{\sqrt{2}}\phi_B^+ + \frac{\not{n}_-}{\sqrt{2}}\phi_B^- \right), \quad (10)$$

where ϕ_B^\pm are two leading-twist distribution amplitudes with different asymptotic behaviors, which obey the normalizations

$$\int_0^1 \phi_B^\pm(y)dy = \frac{f_B}{2\sqrt{2N_c}}. \quad (11)$$

By using the identity $(\not{q} + M)\gamma_5(1 + \frac{\not{n}_+}{\sqrt{2}} + \frac{\not{n}_-}{\sqrt{2}}) = 0$, Eq.(10) can be written as

$$\Phi_B = -\frac{i}{\sqrt{2N_c}}(\not{q} + M)\gamma_5 \left(\phi_B^- + \frac{\not{n}_+}{\sqrt{2}}(\phi_B^- - \phi_B^+) \right), \quad (12)$$

which corresponds to the choice of q_1 as shown in Eq. (4) [62]. In this case, $\phi_B = \phi_B^-$ is the leading component and $\bar{\phi}_B = \phi_B^- - \phi_B^+$ the subleading one. It has been pointed out that the subleading component contribution is power suppressed, thus its contribution can be neglected compared to that of leading one [29]. However, the recent updated studies on the nonleptonic B decays show the subleading contribution are in fact comparable with those from the next-to-leading order corrections [63, 64]. In the following analysis we also consider this power-suppressed contribution and investigate its influence on baryonic B decays. For numerical estimation, we use the conventional Gaussian model [29]

$$\phi_B^-(y, b_q) = N_B y^2 (1-y)^2 \exp \left[-\frac{y^2 M^2}{2\omega_b^2} - \frac{\omega_b^2 b_q^2}{2} \right], \quad (13)$$

with b_q being the impact parameter conjugate to the parton transverse momentum q_T . N_B is the normalization constant which related to the B meson decay constant f_B via Eq. (11). We take the shape parameter $\omega_b = 0.40$ GeV for $B_{u,d}$ mesons and $\omega_b = 0.48$ GeV for a B_s meson [65]. ϕ_B^+ can be obtained by solving the equation of motion $\phi_B^- = -y \frac{d\phi_B^+}{dy}$ without three-parton contributions [61], whose explicit expression could be found in [62, 63]. For more alternative models of the B meson DA and the subleading contributions, one can refer to Refs. [66–72].

For decays induced by $b \rightarrow qc\bar{c}$ transition, the related effective Hamiltonian is given by [73]

$$\mathcal{H}_{eff} = \frac{G_F}{\sqrt{2}} \{ V_{cb}V_{cq}^* [C_1(\mu)O_1(\mu) + C_2(\mu)O_2(\mu)] - \sum_{k=3}^{10} V_{tb}V_{tq}^* C_k(\mu)O_k(\mu) \} + \text{H.c.}, \quad (14)$$

with $q = d, s$. G_F is the Fermi constant, and V are the CKM matrix elements, $C_l(\mu)$ are Wilson coefficients at the renormalization scale μ and the four quark operators O_l are

$$\begin{aligned} O_1 &= \bar{c}_i \gamma_\mu (1 - \gamma_5) b_j \otimes \bar{q}_j \gamma^\mu (1 - \gamma_5) c_i, \\ O_2 &= \bar{c}_i \gamma_\mu (1 - \gamma_5) b_i \otimes \bar{q}_j \gamma^\mu (1 - \gamma_5) c_j, \\ O_3 &= \bar{q}_i \gamma_\mu (1 - \gamma_5) b_i \otimes \sum_{q'} \bar{q}'_j \gamma^\mu (1 - \gamma_5) q'_j, \\ O_4 &= \bar{q}_i \gamma_\mu (1 - \gamma_5) b_j \otimes \sum_{q'} \bar{q}'_j \gamma^\mu (1 - \gamma_5) q'_i, \\ O_5 &= \bar{q}_i \gamma_\mu (1 - \gamma_5) b_i \otimes \sum_{q'} \bar{q}'_j \gamma^\mu (1 + \gamma_5) q'_j, \\ O_6 &= \bar{q}_i \gamma_\mu (1 - \gamma_5) b_j \otimes \sum_{q'} \bar{q}'_j \gamma^\mu (1 + \gamma_5) q'_i, \\ O_7 &= \frac{3}{2} \bar{q}_i \gamma_\mu (1 - \gamma_5) b_i \otimes \sum_{q'} e_{q'} \bar{q}'_j \gamma^\mu (1 + \gamma_5) q'_j, \\ O_8 &= \frac{3}{2} \bar{q}_i \gamma_\mu (1 - \gamma_5) b_j \otimes \sum_{q'} e_{q'} \bar{q}'_j \gamma^\mu (1 + \gamma_5) q'_i, \end{aligned}$$

$$\begin{aligned}
O_9 &= \frac{3}{2} \bar{q}_i \gamma_\mu (1 - \gamma_5) b_i \otimes \sum_{q'} e_{q'} \bar{q}'_j \gamma^\mu (1 - \gamma_5) q'_j, \\
O_{10} &= \frac{3}{2} \bar{q}_i \gamma_\mu (1 - \gamma_5) b_j \otimes \sum_{q'} e_{q'} \bar{q}'_j \gamma^\mu (1 - \gamma_5) q'_i.
\end{aligned} \tag{15}$$

The summation of q' runs through u, d, s, c , and b quarks. The decay amplitude of $B \rightarrow \mathcal{B}_c \bar{\mathcal{B}}_c$ can be described by sandwiching \mathcal{H}_{eff} with the initial and final states,

$$\mathcal{M} = \langle \mathcal{B}_c \bar{\mathcal{B}}_c | \mathcal{H}_{eff} | B \rangle = \bar{u} [H_S + H_P \gamma_5] v, \tag{16}$$

where H_S and H_P are the respective S -wave and P -wave invariant amplitudes. They can symbolically be written as

$$H_{S/P} = \frac{16 f_{\mathcal{B}_c} f_{\bar{\mathcal{B}}_c} \pi^2 G_F}{27 \sqrt{3}} \sum_{R_{ij}} \int \mathcal{D}x \mathcal{D}b \alpha_s^2(t_{R_{ij}}) e^{-S_B - S_{\mathcal{B}_c} - S_{\bar{\mathcal{B}}_c}} \Omega_{R_{ij}}(b, b', b_q) \sum_{\sigma=LL, SP} a_{R_{ij}}^\sigma H_{R_{ij}}^{\sigma, S/P}(x, x', y), \tag{17}$$

with the integration measures

$$\begin{aligned}
\mathcal{D}x &= dx_1 dx_2 dx_3 \delta(1 - x_1 - x_2 - x_3) dx'_1 dx'_2 dx'_3 \delta(1 - x'_1 - x'_2 - x'_3) dy, \\
\mathcal{D}b &= d^2 \mathbf{b}_q d^2 \mathbf{b}_2 d^2 \mathbf{b}_3 d^2 \mathbf{b}'_2 d^2 \mathbf{b}'_3.
\end{aligned} \tag{18}$$

The δ functions enforce momentum conservation. $a_{R_{ij}}^\sigma$ denotes the product of the CKM matrix elements and the Wilson coefficients, and the labels $\sigma = LL$ and SP refer to the contributions from $(V - A)(V - A)$ and $(S - P)(S + P)$ operators, respectively. $H_{R_{ij}}^\sigma$ is the numerator of the hard amplitude depending on the spin structure of final state. $\Omega_{R_{ij}}$ is the Fourier transformation of the denominator of the hard amplitude from the k_T space to its conjugate b space. The involving variables b, b' and b_q conjugate to the parton transverse momenta k_T, k'_T and q_T , respectively. The hard scale t for each diagram is chosen as the maximal virtuality of internal particles including the factorization scales in a hard amplitude:

$$t_{R_{ij}} = \max(\sqrt{|t_A|}, \sqrt{|t_B|}, \sqrt{|t_C|}, \sqrt{|t_D|}, w, w', 1/b_q), \tag{19}$$

where $t_{A,B}$ are relevant to the two virtual quarks, while $t_{C,D}$ are associated with the two hard gluons. The infrared cut $w^{(\prime)}$ is chosen to be the smallest inverse of a typical transverse distance among three valence quarks in baryon [36]. Those quantities associated with specific diagram, such as $a_{R_{ij}}$, $H_{R_{ij}}$, and $t_{R_{ij}}$, are collected in Appendix.

The Sudakov exponents associated with the initial and final states are written as [31, 40, 74]

$$\begin{aligned}
S_B &= s(q_1^-, b_q) + \frac{5}{3} \int_{1/b_q}^t d\bar{\mu} \frac{\gamma(\alpha_s(\bar{\mu}))}{\bar{\mu}} \\
S_{\mathcal{B}_c} &= s_c(k_1'^-, cw') + \sum_{l=2}^3 s(k_l'^-, cw') + \frac{8}{3} \int_{cw'}^t d\bar{\mu} \frac{\gamma(\alpha_s(\bar{\mu}))}{\bar{\mu}} \\
S_{\bar{\mathcal{B}}_c} &= s_c(k_1^+, cw) + \sum_{l=2}^3 s(k_l^+, cw) + \frac{8}{3} \int_{cw}^t d\bar{\mu} \frac{\gamma(\alpha_s(\bar{\mu}))}{\bar{\mu}}
\end{aligned} \tag{20}$$

with the quark anomalous dimension $\gamma(\alpha_s(\bar{\mu})) = -\alpha_s(\bar{\mu})/\pi$. Here we have included the Sudakov exponent s_c associated with the charm quark, which carries large longitudinal momentum in the fast recoil region [37]. Its explicit form with the inclusion of finite charm quark mass effects can be found in Ref [75]. The exponent s for an energetic light quark is referred to Refs [31, 36]. The coefficient of the quark anomalous dimension in Eq. (20) is set to $5/3(8/3)$ for heavy meson (baryon) because the rescaled heavy-quark field adopted in the definition of the heavy hadron wave function has a self-energy correction different from that of the full heavy-quark field [76]. We assign a coefficient c in front of $\omega^{(\prime)}$ to mimic theoretical uncertainties in resummation. Its value is expected to be of $\mathcal{O}(1)$ and is allowed to deviate slightly from unity. The best fit to the experimental data of $\mathcal{B}(B^- \rightarrow \Xi_c^0 \bar{\Lambda}_c^-)$ determines the parameter as $c = 1.05$, which is close to $c = 1.14$ for the proton one [74].

III. NUMERICAL RESULTS

We perform the numerical analysis in this section based on the factorization formulas derived above. The default values for input parameters are given as follows:

- Wolfenstein parameters [17]: $\lambda = 0.22650$, $A = 0.790$, $\bar{\rho} = 0.141$, $\bar{\eta} = 0.357$.
- lifetimes (ps) [17]: $\tau_{B_s} = 1.51$, $\tau_{B_d} = 1.52$, $\tau_{B_u} = 1.638$.
- Masses (GeV) [17]: $M_{B_{u,d}} = 5.28$, $M_{B_s} = 5.37$, $m_{\Lambda_c} = 2.286$, $m_{\Xi_c} = 2.47$, $m_b = 4.8$, $m_c = 1.275$.
- Decay constants [33, 49, 59]: $f_{B_{u,d}} = 0.19$ GeV, $f_{B_s} = 0.24$ GeV, $f_{\Lambda_c} = 0.022$ GeV³, $f_{\Xi_c} = 0.027$ GeV³.

Other nonperturbative parameters appearing in the hadron LCDAs have been specified in the preceding section.

TABLE II: Invariant amplitudes from the leading-twist (ϕ_B) and subleading-twist ($\bar{\phi}_B$) B meson LCDAs. The last column is their sum.

Mode	Type	Amplitude	ϕ_B	$\bar{\phi}_B$	$\phi_B + \bar{\phi}_B$
$B^- \rightarrow \Xi_c^0 \bar{\Lambda}_c^-$	C	H_S	$1.2 \times 10^{-7} + i8.3 \times 10^{-9}$	$2.0 \times 10^{-8} + i3.2 \times 10^{-8}$	$1.4 \times 10^{-7} + i4.0 \times 10^{-8}$
		H_P	$-7.8 \times 10^{-9} + i4.9 \times 10^{-8}$	$-1.0 \times 10^{-8} + i1.5 \times 10^{-8}$	$-1.8 \times 10^{-8} + i6.4 \times 10^{-8}$
		$ \mathcal{M} (\text{GeV})$	3.7×10^{-7}	1.3×10^{-7}	4.8×10^{-7}
$\bar{B}_s^0 \rightarrow \Lambda_c^+ \bar{\Lambda}_c^-$	E	H_S	$4.8 \times 10^{-9} - i1.1 \times 10^{-8}$	$5.0 \times 10^{-9} + i8.6 \times 10^{-9}$	$9.8 \times 10^{-9} - i2.4 \times 10^{-9}$
		H_P	$-9.6 \times 10^{-10} + i1.9 \times 10^{-8}$	$5.8 \times 10^{-9} - i3.0 \times 10^{-9}$	$4.8 \times 10^{-9} + i1.6 \times 10^{-8}$
		$ \mathcal{M} (\text{GeV})$	1.1×10^{-7}	4.5×10^{-8}	9.5×10^{-8}
$\bar{B}^0 \rightarrow \Lambda_c^+ \bar{\Lambda}_c^-$	$C + E$	H_S	$7.8 \times 10^{-9} + i6.1 \times 10^{-9}$	$1.0 \times 10^{-10} + i1.7 \times 10^{-9}$	$7.9 \times 10^{-9} + i7.8 \times 10^{-9}$
		H_P	$-2.5 \times 10^{-9} + i1.5 \times 10^{-9}$	$-2.8 \times 10^{-9} + i2.3 \times 10^{-9}$	$-5.3 \times 10^{-9} + i3.8 \times 10^{-9}$
		$ \mathcal{M} (\text{GeV})$	3.0×10^{-8}	2.0×10^{-8}	4.5×10^{-8}

We first compare the numerical results of the invariant amplitudes from the leading component (ϕ_B) and subleading component ($\bar{\phi}_B$) of the B meson LCDAs in Table II. The dominant topologies contributing to these decays are also indicated in the second column through the symbols C (the internal W -emission) and E (the W -exchange). It is observed that the subleading contributions are in fact comparable with the leading ones, so the interference between the leading and subleading amplitudes has a significant impact on the magnitude of amplitudes. Table II illustrates that the interference patterns for C and E amplitudes differ, with the former being constructive and the latter destructive. The $\bar{B}^0 \rightarrow \Lambda_c^+ \bar{\Lambda}_c^-$ decay amplitude receives contributions from C and E type topologies with the former as the main contribution. The resulting interference is also constructive. It appears that the subleading contributions from $\bar{\phi}_B$ can reach as much as (30 – 70)% of leading ones for the baryonic B decays under consideration, which are larger than 30% in the mesonic B decays [30, 63, 64]. The inclusion of subleading correction can enhance the total amplitudes $|\mathcal{M}(B^- \rightarrow \Xi_c^0 \bar{\Lambda}_c^-)|$ and $|\mathcal{M}(\bar{B}^0 \rightarrow \Lambda_c^+ \bar{\Lambda}_c^-)|$ by a factor of 1.3 and 1.5, respectively, and lower $|\mathcal{M}(\bar{B}_s^0 \rightarrow \Lambda_c^+ \bar{\Lambda}_c^-)|$ by a factor of 0.9 as shown in Table II. We will see later that this subleading corrections improve the consistency between the PQCD predictions and the experimental data of the $B^- \rightarrow \Xi_c^0 \bar{\Lambda}_c^-$ decays. We then conclude that the effect of the subleading component of the B meson distribution amplitude is indeed substantial for the concerned decays, which warns us that it is worth reexamining the doubly-charmed mesonic B decays with the PQCD approach by considering the subleading component $\bar{\phi}_B$ in the future.

We present the contributions to the amplitudes from various twist combinations of the baryon and antibaryon LCDAs in Table III, in which both ϕ_B and $\bar{\phi}_B$ contributions from B meson LCDAs have been included. The twists in the rows correspond to the baryon LCDAs and those in the columns to the antibaryon ones. We learn from Table III that the higher-twist baryon LCDAs give significant contributions to the decay amplitudes of all the three modes. For example, the contributions from the combination of twist-3 baryon and twist-3 antibaryon LCDAs dominate the decay amplitudes, while the leading-twist contributions are generally an order of magnitude smaller. The main reason, as stated in Ref. [41], is due to the endpoint enhancement behaviors caused by the higher-twist baryon LCDAs, which could overcome the power suppressions from r or \bar{r} and remarkably increase higher-twist contributions. Although the contributions of the twist-4-twist-4 combination are also important, they are still less than the dominant twist-3-twist-3 combination, indicating the reliability of twist expansion of the baryon LCDAs. As displayed in Table III, the contributions from the combination of twist-3 baryon (antibaryon) and twist-2 or 4 antibaryon (baryon) LCDAs in $\bar{B}_s^0 \rightarrow \Lambda_c^+ \bar{\Lambda}_c^-$ mode vanish. This observation can be understood easily as follows. According to the general definition of the non-local matrix elements in Eq. (5), the even (odd) twist LCDAs are always accompanied by even (odd) number of Dirac matrices. Therefore, the combination of baryon and antibaryon LCDAs with opposite parity always contains odd numbers of Dirac matrices, which must be exactly zero in a trace calculation. This situation appears in the W -exchange diagrams, in which a contraction of light quark spinor indices leads to a trace involving both baryon and antibaryon LCDAs.

TABLE III: Magnitude of amplitude $|\mathcal{M}|(\text{GeV})$ from various twist combinations of the baryon and antibaryon LCDAs.

	Twist-2	Twist-3	Twist-4
$B^- \rightarrow \Xi_c^0 \bar{\Lambda}_c^-$			
Twist-2	3.5×10^{-8}	1.7×10^{-7}	9.6×10^{-8}
Twist-3	1.4×10^{-7}	1.9×10^{-7}	1.4×10^{-7}
Twist-4	1.1×10^{-7}	2.0×10^{-7}	1.6×10^{-7}
$\bar{B}_s^0 \rightarrow \Lambda_c^+ \bar{\Lambda}_c^-$			
Twist-2	3.2×10^{-9}	0	1.5×10^{-7}
Twist-3	0	1.5×10^{-7}	0
Twist-4	5.8×10^{-8}	0	1.5×10^{-8}
$\bar{B}^0 \rightarrow \Lambda_c^+ \bar{\Lambda}_c^-$			
Twist-2	5.0×10^{-9}	2.6×10^{-8}	4.1×10^{-8}
Twist-3	2.1×10^{-8}	5.0×10^{-8}	1.5×10^{-8}
Twist-4	2.4×10^{-8}	3.0×10^{-8}	2.4×10^{-8}

TABLE IV: Theoretical predictions and experimental results on branching ratios of $B \rightarrow \mathcal{B}_c \bar{\mathcal{B}}_c$ decays. The label PQCD-I means the PQCD results without the subleading correction from the B meson LCDAs, and PQCD-II means the inclusions of the subleading correction. The errors for these entries correspond to the uncertainties in the B meson LCDAs, charmed baryon LCDAs, the scale dependence, and the Sudakov resummation, respectively. The model predictions by SU(3) [28] are also displayed here for comparison. The last column contains measured branching ratios or upper limits from the Particle Data Group (PDG) [17] or the original experimental literature [21–23].

Mode	Transition	PQCD-I	PQCD-II	SU(3) [28]	Data [17, 21–23]
$B^- \rightarrow \Xi_c^0 \bar{\Lambda}_c^-$	$b \rightarrow sc\bar{c}$	$(5.7_{-1.6}^{+2.3} - 2.5_{-0.9}^{+1.9} - 0.6_{-0.6}^{+1.1}) \times 10^{-4}$	$(9.5_{-2.3}^{+3.0} - 3.5_{-3.5}^{+2.6} - 1.4_{-1.1}^{+1.7}) \times 10^{-4}$	$7.8_{-2.0}^{+2.3} \times 10^{-4}$	$(9.5 \pm 2.3) \times 10^{-4}$
$\bar{B}^0 \rightarrow \Xi_c^+ \bar{\Lambda}_c^-$	$b \rightarrow sc\bar{c}$	$(5.3_{-1.4}^{+2.1} - 2.2_{-0.8}^{+1.7} - 0.6_{-0.6}^{+1.0}) \times 10^{-4}$	$(8.8_{-2.1}^{+2.7} - 3.1_{-3.1}^{+2.6} - 1.2_{-1.0}^{+1.5}) \times 10^{-4}$	$7.2_{-1.9}^{+2.1} \times 10^{-4}$	$(12 \pm 8) \times 10^{-4}$
$\bar{B}_s^0 \rightarrow \Lambda_c^+ \bar{\Lambda}_c^-$	$b \rightarrow sc\bar{c}$	$(5.0_{-0.6}^{+0.7} - 0.5_{-0.5}^{+0.3} - 0.9_{-1.0}^{+1.4}) \times 10^{-5}$	$(4.0_{-0.3}^{+0.7} - 0.1_{-0.1}^{+0.2} - 0.7_{-0.8}^{+0.9}) \times 10^{-5}$	$8.1_{-1.5}^{+1.7} \times 10^{-5}$	$< 9.9 \times 10^{-5}$
$\bar{B}^0 \rightarrow \Lambda_c^+ \bar{\Lambda}_c^-$	$b \rightarrow dc\bar{c}$	$(4.0_{-1.4}^{+2.5} - 1.3_{-1.3}^{+1.7} - 0.6_{-0.4}^{+0.6}) \times 10^{-6}$	$(8.8_{-2.8}^{+4.4} - 3.6_{-3.6}^{+3.5} - 0.9_{-0.6}^{+1.1}) \times 10^{-6}$	$2.1_{-0.8}^{+1.0} \times 10^{-5}$	$< 1.6 \times 10^{-5}$

Using above numerical result of the decay amplitudes, it is straightforward to calculate the branching ratio, reads

$$\mathcal{B} = \frac{P_c \tau_B}{8\pi M^2} |\mathcal{M}|^2 = \frac{P_c \tau_B}{8\pi M^2} (|H_S|^2 Q_+ + |H_P|^2 Q_-), \quad (21)$$

with $Q_{\pm} = M^2 - (m \pm \bar{m})^2$ and the spatial momentum of baryon $P_c = \sqrt{Q_+ Q_-} / (2M)$. The corresponding numerical results are summarized in Table IV. The results without (with) the subleading contribution, labeled by PQCD-I(II), are also shown for comparison. Four types of theoretical uncertainties are estimated here. The first error is due to the shape parameter ω_b in the B meson distribution amplitudes. We consider the variation of its shape parameter within 10% around its central value. The resulting uncertainty for the branching ratios amount to 20% – 50%. The second error bar includes the uncertainties due to variation of the Gegenbauer moments in the charmed baryon LCDAs as displayed in Table I, added in quadrature. Numerical results demonstrate that the branching ratios are more sensitive to $a_2^{(3)}$ among these nonperturbative parameters. The third one reflects the unknown next-to-leading-order QCD corrections characterized by the hard scale t , which is varied from $0.8t$ to $1.2t$. The last uncertainty is due to the parameter $c = 1.05 \pm 0.05$ in the Sudakov resummation for the charmed baryon wave function. The variation of c denotes the different partitions of radiative corrections into the perturbative Sudakov factor and the nonperturbative wave function [36]. It is concluded that the absolute branching ratios suffer large theoretical uncertainties from the nonperturbative hadronic parameters in the present situation.

Predictions in the SU(3) approach [28] and the data from the Particle Data Group [17] are also collected in Table IV to make a comparison. On the experimental side, Belle collaboration has published the measurements of $\mathcal{B}(B^- \rightarrow \Xi_c^0 \bar{\Lambda}_c^-) = (9.51 \pm 2.10 \pm 0.88) \times 10^{-4}$ [21] and $\mathcal{B}(\bar{B}^0 \rightarrow \Xi_c^+ \bar{\Lambda}_c^-) = (1.16 \pm 0.42 \pm 0.15) \times 10^{-3}$ [22], where the first uncertainty is statistical and the second is systematic. The 95% credibility level upper limits on $\bar{B}^0 \rightarrow \Lambda_c^+ \bar{\Lambda}_c^-$ and $\bar{B}_s^0 \rightarrow \Lambda_c^+ \bar{\Lambda}_c^-$ were determined to be 1.6×10^{-5} and 9.9×10^{-5} by LHCb [23], respectively. However, the previous measurement performed by Belle yields a larger value of $\mathcal{B}(\bar{B}^0 \rightarrow \Lambda_c^+ \bar{\Lambda}_c^-) = (2.2_{-1.6}^{+2.2} \pm 1.3) \times 10^{-5}$ [77] with an upper limit of 6.2×10^{-5} at 90% confidence level. In the SU(3) approach [28], the W -emission and W -exchange amplitudes

are determined using above available experimental data, which can be applied to explore other channels based on the SU(3) flavour symmetry. As indicated in Table IV, the PQCD predictions without the subleading corrections are generally smaller than the SU(3) results and the data. As aforementioned, the interference patterns between the leading and subleading contributions from the B meson LCDAs are different for the C and E amplitudes. After including the subleading corrections, the predicted branching ratios of $B^- (\bar{B}^0) \rightarrow \Xi_c^0 (\Xi_c^+) \bar{\Lambda}_c^-$ and $\bar{B}_s^0 \rightarrow \Lambda_c^+ \bar{\Lambda}_c^-$ will increase and decrease, respectively. Roughly speaking, the inclusion of the subleading corrections could alleviate the discrepancy and improve the agreement with the current data. In particular, our prediction on the branching ratio of $B^- \rightarrow \Xi_c^0 \bar{\Lambda}_c^-$ is compatible with the world average value. It is worth mentioning that the tuning of c is not crucial for explaining the data because of the insensitivity of the predictions to c shown in Table IV. The PQCD predictions for the $\mathcal{B}(\bar{B}^0 \rightarrow \Lambda_c^+ \bar{\Lambda}_c^-)$ and $\mathcal{B}(\bar{B}_s^0 \rightarrow \Lambda_c^+ \bar{\Lambda}_c^-)$ branching ratios reach half of the measured upper limits. They may be just around the corner. Confronting with the results of SU(3) approach [28], our branching ratios for the first two modes are larger, however those of the last two processes are smaller. Nevertheless, considering the uncertainties of the two theoretical predictions, the disparities are not serious. An earlier calculation in Ref. [25] gave $\mathcal{B}(B^- \rightarrow \Xi_c^0 \bar{\Lambda}_c^-) = (2.2_{-0.6}^{+0.6+5.1+6.1}) \times 10^{-3}$ and $\mathcal{B}(\bar{B}^0 \rightarrow \Xi_c^+ \bar{\Lambda}_c^-) = (2.0_{-0.6}^{+0.5+4.7+5.6}) \times 10^{-3}$, which are considerably larger. Although the subsequent updated branching ratios for the two modes are consistent with ours, their central value of $\mathcal{B}(\bar{B}^0 \rightarrow \Lambda_c^+ \bar{\Lambda}_c^-) = (5.2_{-1.1}^{+2.3+0.6+2.6+0.0}) \times 10^{-5}$ [26] exceeds the current existing upper limit by a factor of 3.

TABLE V: Contributions to the invariant amplitudes of the $\bar{B}^0 \rightarrow \Lambda_c^+ \bar{\Lambda}_c^-$ decay from C and E topologies. The last two columns are their relative magnitude and phase, respectively.

Amplitude	C	E	$ \frac{E}{C} $	$\text{Arg}(E/C)$
H_S	$1.0 \times 10^{-8} + i7.5 \times 10^{-9}$	$-2.3 \times 10^{-9} + i3.0 \times 10^{-10}$	0.18	2.37
H_P	$-4.1 \times 10^{-9} + i7.4 \times 10^{-9}$	$-1.1 \times 10^{-9} - i3.7 \times 10^{-9}$	0.44	2.34

The decay $\bar{B}^0 \rightarrow \Lambda_c^+ \bar{\Lambda}_c^-$ is of particular interest as it receives both the W -emission and W -exchange contributions. In the SU(3) approach, the magnitudes of the two topological amplitudes were determined to be $|C| = 1.29 \pm 0.18 \text{ GeV}^3$ and $|E| = 0.20 \pm 0.02 \text{ GeV}^3$ [28]. The resultant ratio of $|2E/C| = 0.31$ indicates the W -exchange contribution is important and nonnegligible. As pointed out in [28], the accuracy of the current available data is not high enough to determine the W -exchange amplitude and the relative phase between the W -emission and W -exchange amplitudes simultaneously. To accommodate the experimental data, the relative phase was chosen as π to maximize the destructive interference between the W -emission and W -exchange amplitudes. The PQCD predictions on the central values of the invariant amplitudes from the W -emission and W -exchange diagrams are presented separately in Table V, where the last two columns are the relative magnitude and phase, respectively. It should be noted that the topological amplitudes defined in [28] do not contain the Fermi coupling constant and CKM matrix elements, so we cannot compare directly the respective topological amplitudes with theirs except for the relative ratio. It is obvious that the relative sizes of the two topological amplitudes have different pattern in the two invariant amplitudes H_S and H_P . The PQCD prediction on $|E/C|$ for $H_{S(P)}$ is smaller (larger) than that of SU(3). The calculated relative phases are around 2.3 rad, implies the interferences between C and E amplitudes are indeed destructive, and support the assumption made in Ref [28]. Nevertheless, the somewhat deviation from π in our calculations implies the destructive interferences are not at the maximum.

As stressed in [28], if the W -exchange contribution is dropped, the measured upper limit of $\mathcal{B}(\bar{B}^0 \rightarrow \Lambda_c^+ \bar{\Lambda}_c^-)$ is significantly below a naive extrapolation from $\mathcal{B}(B^- \rightarrow \bar{\Lambda}_c^- \Xi_c^0)$ assuming a simple Cabibbo-suppression factor of $|V_{cd}/V_{cs}|^2$. Then they argued that a destructive interfering effect between the W -exchange and W -emission amplitudes can reduce the overestimated branching ratio to accommodate the measurement. However, this explanation seem to be not sufficient, because their central value still saturates the experimental upper bound slightly as exhibited in Table IV in spite of considering a maximum destructive interference. In this case, a way out is to consider SU(3) breaking effect since the small energy release in the doubly-charmed baryonic B decays is not enough to weaken the differences among the SU(3) multiplets. At the hadron level, SU(3) flavor breaking due to the strange and light quark differences will manifest in the baryon masses, decay constants, and baryonic LCDAs in our calculations. When the W -exchange contribution is turned off, we obtain the central value of branching ratio $\mathcal{B}(\bar{B}^0 \rightarrow \Lambda_c^+ \bar{\Lambda}_c^-) = 1.3 \times 10^{-5}$, which is still below the upper bound. When the W -exchange contribution is turned on, the calculated value further reduces to 8.8×10^{-6} owing to the aforementioned destructive interference. We thereby point out that the SU(3) symmetry breaking as well as the interference effect play an essential role in understanding the measurements of $\mathcal{B}(\bar{B}^0 \rightarrow \Lambda_c^+ \bar{\Lambda}_c^-)$ and $\mathcal{B}(B^- \rightarrow \Xi_c^0 \bar{\Lambda}_c^-)$. The significant SU(3) breaking effect can also explain why our value is lower than the SU(3) one by a factor 2.

TABLE VI: Asymmetry parameters for the considered decays. The theoretical uncertainties are the same as for branching ratios in Table IV.

Mode	α	β	γ
$B^- \rightarrow \Xi_c^0 \bar{\Lambda}_c^-$	$-0.01^{+0.10+0.12+0.05+0.01}_{-0.10-0.29-0.14-0.01}$	$-0.99^{+0.01+0.09+0.00+0.00}_{-0.00-0.01-0.00-0.00}$	$-0.07^{+0.07+0.38+0.04+0.07}_{-0.06-0.13-0.05-0.08}$
$\bar{B}_s^0 \rightarrow \Lambda_c^+ \bar{\Lambda}_c^-$	$-0.03^{+0.05+0.03+0.05+0.01}_{-0.04-0.04-0.03-0.00}$	$-0.57^{+0.02+0.02+0.00+0.05}_{-0.03-0.02-0.02-0.05}$	$-0.82^{+0.03+0.02+0.01+0.04}_{-0.01-0.01-0.00-0.03}$
$\bar{B}^0 \rightarrow \Lambda_c^+ \bar{\Lambda}_c^-$	$0.17^{+0.08+0.08+0.03+0.02}_{-0.08-0.05-0.18-0.01}$	$-0.97^{+0.04+0.06+0.02+0.02}_{-0.03-0.00-0.02-0.01}$	$-0.15^{+0.17+0.54+0.14+0.09}_{-0.14-0.16-0.11-0.11}$

We next turn to some interesting asymmetry parameters in the decays under consideration, defined by [78]

$$\alpha = \frac{|H_+|^2 - |H_-|^2}{|H_+|^2 + |H_-|^2}, \quad \beta = \frac{2Im(H_+H_-^*)}{|H_+|^2 + |H_-|^2}, \quad \gamma = \frac{2Re(H_+H_-^*)}{|H_+|^2 + |H_-|^2}, \quad (22)$$

with $H_{\pm} = \frac{1}{\sqrt{2}}(\sqrt{Q_+}H_S \mp \sqrt{Q_-}H_P)$. α is the up-down asymmetry parameter. β is a naively T -odd observable. They are both P -odd, while γ is P -even. They are related by the identity $\alpha^2 + \beta^2 + \gamma^2 = 1$. Our results on these asymmetries are summarized in Table VI, where the uncertainties are from the same quantities as above. The most important source of the theoretical errors is the assumption of the heavy quark limit for the heavy baryon LCDAs. We remark that the uncertainties due to the baryon LCDAs may be exaggerated because the parameters used here are actually for bottom baryons rather than charmed baryons, which are not known at present. Any significant reduction of the error requires more accurate information on the charmed baryon LCDAs. As these asymmetries received less theoretical and experimental attentions, our predictions can be compared in future.

IV. CONCLUSION

Baryonic B decays offer alternative robust ways to test the SM and search for new physics, complementing searches with mesonic B -decays. However, the QCD dynamics of baryonic B decay processes are more complicated than those of mesonic ones and poorly understood theoretically. In particular, the quantitative analyses on the baryonic B decays based on the QCD-inspired approaches are still not developed. In this work, we limit our attention to the four observed two-body doubly charmed baryonic B decays and make the first steps to calculate their decay branching ratios and asymmetry parameters in the framework of PQCD. Our results could be helpful for a future experimental search for them and provide deeper insights in the understanding of the dynamics of baryonic B decay processes.

From the previous argument that the energy release in the doubled-charmed two-body decay is small, in order to improve the theoretical calculation accuracy, some higher-power corrections arise from the nonperturbative hadron distribution amplitudes are taken into account in our numerical analysis. The subleading contribution of the B meson distribution amplitude and the charmed baryon light-cone distribution amplitudes up to the twist-4 level are considered for the processes in question. It is found that the effect of the subleading component of the B meson distribution amplitude is indeed essential and cannot be neglected. The subleading contributions can interfere destructively or constructively with the leading ones. Contributions to the decay amplitude from various twist combinations of the baryon and antibaryon LCDAs are elaborated. It is clear that the higher-twist baryon LCDAs give the dominant contribution to the decay amplitudes of all the four modes.

With the decay amplitudes, we predict the decay branching ratios and asymmetry parameters, where the theoretical uncertainties arise from the nonperturbative hadronic LCDAs, the Sudakov resummation, and the hard scales. The accuracy of the theoretical predictions can be systematically improved once the charmed baryon LCDAs are available in the future. Our prediction on the branching ratio of $B^- \rightarrow \Xi_c^0 \bar{\Lambda}_c^-$ is compatible with the world average value, while the values of $\mathcal{B}(\bar{B}^0 \rightarrow \Lambda_c^+ \bar{\Lambda}_c^-)$ and $\mathcal{B}(\bar{B}_s^0 \rightarrow \Lambda_c^+ \bar{\Lambda}_c^-)$ satisfy the existing experimental bounds. We also compare the calculated decay branching ratios with those from other theoretical approaches when they are available. It is discovered that various results span wide ranges, which call for more precise measurements to discriminate them. The asymmetry parameters are investigated for the first time in this work. As the asymmetries have received less attentions in the literature, we await future comparisons.

We emphasize that the SU(3) breaking effects are crucial in explaining the measured branching ratios of $\mathcal{B}(\bar{B}^0 \rightarrow \Lambda_c^+ \bar{\Lambda}_c^-)$ and $\mathcal{B}(B^- \rightarrow \Xi_c^0 \bar{\Lambda}_c^-)$. An explicit study of the SU(3) breaking effects to other double charmed baryonic B decays in PQCD is in progress.

Acknowledgments

We would like to acknowledge Professor Hsiang-nan Li and Professor Yu-Kuo Hsiao for helpful discussions. This work is supported by National Natural Science Foundation of China under Grants Nos. 12075086, 12375089 and 12435004. Z.R. is also supported in part by the Natural Science Foundation of Hebei Province under Grant No. A2021209002 and No. A2019209449. Z.T.Z. is supported by the Natural Science Foundation of Shandong province under the Grant No. ZR2022MA035. Y.Li is also supported by the Natural Science Foundation of Shandong province under the Grant No. ZR2022ZD26.

Appendix A: FACTORIZATION FORMULAS

In this appendix, we give the expressions of those quantities associated with specific diagram entering to the decay amplitude in Eq. (17). The expressions of a^σ , $\Omega_{R_{ij}}$, and $t_{A,B,C,D}$ are given in Tables VII, VIII, and IX, respectively. The auxiliary functions h_l in Table VIII can be found in [42].

In the present work, the formulas of $H_{R_{ij}}^\sigma(x, x', y)$ are rather lengthy due to many higher twist contributions are included. Here, we only show some details for diagrams Fig. 1 (b6) and Fig. 2 (c7), which represent the main contributions in each topology. The others can be derived in a similar way.

For the S -wave expressions of Fig. 1 (b6):

$$\begin{aligned}
H_{C_{b6}}^{LL,S}(x, x', y) = & \frac{M^3}{f^- - f^+} (\bar{r}x_1x_2(2\phi_B(\bar{\phi}_3^a + \bar{\phi}_3^s - 2\bar{\phi}_4)\phi_3^s + 2\bar{\phi}_4\bar{\phi}_B\phi_3^s + \phi_2\phi_B\bar{\phi}_2 + \phi_2(\bar{\phi}_3^a - \bar{\phi}_3^s)(2\phi_B - \bar{\phi}_B))(f^+)^2 \\
& + (r(2\bar{\phi}_2\bar{\phi}_B\phi_3^s - \phi_B(-2\phi_3^s\bar{\phi}_3^a + \phi_4\bar{\phi}_3^a + 2\phi_3^s\bar{\phi}_3^s + \phi_4\bar{\phi}_3^s + 2\phi_3^s\bar{\phi}_2 + \phi_4\bar{\phi}_4) + \phi_4(\bar{\phi}_3^a + \bar{\phi}_3^s)\bar{\phi}_B)(x'_2 + x'_3) \\
& - \bar{r}\bar{\phi}_B(x_2(2(\bar{\phi}_3^a + \bar{\phi}_3^s)\phi_3^s + \phi_2\bar{\phi}_2) + (2\bar{\phi}_2\phi_3^s + \phi_4(\bar{\phi}_3^a + \bar{\phi}_3^s))(x'_2 + x'_3)) \\
& + \bar{r}\phi_B(2x_2(\bar{\phi}_3^a + \bar{\phi}_3^s + \bar{\phi}_4)\phi_3^s + x_2\phi_2(-\bar{\phi}_3^a + \bar{\phi}_3^s + \bar{\phi}_2) \\
& + (-2\phi_3^s\bar{\phi}_3^a + \phi_4\bar{\phi}_3^a + 2\phi_3^s\bar{\phi}_3^s + \phi_4\bar{\phi}_3^s + 2\phi_3^s\bar{\phi}_2 + \phi_4\bar{\phi}_4)(x'_2 + x'_3))f^+ \\
& + \bar{r}(2\bar{\phi}_2\bar{\phi}_B\phi_3^s - \phi_B((\phi_4 - 2\phi_3^s)\bar{\phi}_3^a + 2\phi_3^s\bar{\phi}_3^s + \phi_4\bar{\phi}_3^s + 2\phi_3^s\bar{\phi}_2 + \phi_4\bar{\phi}_4) + \phi_4(\bar{\phi}_3^a + \bar{\phi}_3^s)\bar{\phi}_B)(x'_2 + x'_3) \\
& + f^-((r - \bar{r})x_1x_2(2\phi_B(\bar{\phi}_3^a + \bar{\phi}_3^s - 2\bar{\phi}_4)\phi_3^s + 2\bar{\phi}_4\bar{\phi}_B\phi_3^s + \phi_2\phi_B\bar{\phi}_2 + \phi_2(\bar{\phi}_3^a - \bar{\phi}_3^s)(2\phi_B - \bar{\phi}_B))(f^+)^2 \\
& + (r - \bar{r})(x_2\phi_B(2(\bar{\phi}_3^a + \bar{\phi}_3^s + \bar{\phi}_4)\phi_3^s + \phi_2(-\bar{\phi}_3^a + \bar{\phi}_3^s + \bar{\phi}_2)) - x_2(2(\bar{\phi}_3^a + \bar{\phi}_3^s)\phi_3^s + \phi_2\bar{\phi}_2)\bar{\phi}_B \\
& + (2\bar{\phi}_2(\phi_B - \bar{\phi}_B)\phi_3^s + \phi_B((\phi_4 - 2\phi_3^s)\bar{\phi}_3^a + 2\phi_3^s\bar{\phi}_3^s + \phi_4(\bar{\phi}_3^s + \bar{\phi}_4)) - \phi_4(\bar{\phi}_3^a + \bar{\phi}_3^s)\bar{\phi}_B)(x'_2 + x'_3))f^+ \\
& + \bar{r}(2\bar{\phi}_2(\phi_B - \bar{\phi}_B)\phi_3^s + \phi_B((\phi_4 - 2\phi_3^s)\bar{\phi}_3^a + 2\phi_3^s\bar{\phi}_3^s + \phi_4(\bar{\phi}_3^s + \bar{\phi}_4)) - \phi_4(\bar{\phi}_3^a + \bar{\phi}_3^s)\bar{\phi}_B)(x'_2 + x'_3)), \tag{A1}
\end{aligned}$$

where $\bar{\phi}_{2,3,4}$ denote the corresponding quantities for an antibaryon.

$$\begin{aligned}
H_{C_{b6}}^{SP,S}(x, x', y) = & -\frac{M^3}{2(f^- - f^+)} (\bar{r}x_1x_2(2(\phi_B(\bar{\phi}_3^a + \bar{\phi}_3^s - 2\bar{\phi}_4) + \bar{\phi}_4\bar{\phi}_B)\phi_3^s + \phi_2\phi_B\bar{\phi}_2 + \phi_2(\bar{\phi}_3^a - \bar{\phi}_3^s)(2\phi_B - \bar{\phi}_B))(f^+)^2 \\
& + r((2\bar{\phi}_2\phi_3^s + \phi_4(\bar{\phi}_3^a + \bar{\phi}_3^s))\bar{\phi}_B - \phi_B((\phi_4 - 2\phi_3^s)\bar{\phi}_3^a + 2\phi_3^s\bar{\phi}_3^s + \phi_4\bar{\phi}_3^s + 2\phi_3^s\bar{\phi}_2 + \phi_4\bar{\phi}_4))(x'_2 + x'_3)f^+ \\
& + \bar{r}(x_2(2\phi_B(\bar{\phi}_3^a + \bar{\phi}_3^s + \bar{\phi}_4)\phi_3^s - 2(\bar{\phi}_3^a + \bar{\phi}_3^s)\bar{\phi}_B\phi_3^s + \phi_2\phi_B(-\bar{\phi}_3^a + \bar{\phi}_3^s + \bar{\phi}_2) - \phi_2\bar{\phi}_2\bar{\phi}_B) \\
& + (2\bar{\phi}_2(\phi_B - \bar{\phi}_B)\phi_3^s + \phi_B((\phi_4 - 2\phi_3^s)\bar{\phi}_3^a + 2\phi_3^s\bar{\phi}_3^s + \phi_4(\bar{\phi}_3^s + \bar{\phi}_4)) - \phi_4(\bar{\phi}_3^a + \bar{\phi}_3^s)\bar{\phi}_B)(x'_2 + x'_3))f^+ \\
& + \bar{r}((2\bar{\phi}_2\phi_3^s + \phi_4(\bar{\phi}_3^a + \bar{\phi}_3^s))\bar{\phi}_B - \phi_B((\phi_4 - 2\phi_3^s)\bar{\phi}_3^a + 2\phi_3^s\bar{\phi}_3^s + \phi_4\bar{\phi}_3^s + 2\phi_3^s\bar{\phi}_2 + \phi_4\bar{\phi}_4))(x'_2 + x'_3) \\
& + f^-((r - \bar{r})x_1x_2(2(\phi_B(\bar{\phi}_3^a + \bar{\phi}_3^s - 2\bar{\phi}_4) + \bar{\phi}_4\bar{\phi}_B)\phi_3^s + \phi_2\phi_B\bar{\phi}_2 + \phi_2(\bar{\phi}_3^a - \bar{\phi}_3^s)(2\phi_B - \bar{\phi}_B))(f^+)^2 \\
& + (r - \bar{r})(x_2(2\phi_B(\bar{\phi}_3^a + \bar{\phi}_3^s + \bar{\phi}_4)\phi_3^s - 2(\bar{\phi}_3^a + \bar{\phi}_3^s)\bar{\phi}_B\phi_3^s + \phi_2\phi_B(-\bar{\phi}_3^a + \bar{\phi}_3^s + \bar{\phi}_2) - \phi_2\bar{\phi}_2\bar{\phi}_B) \\
& + (2\bar{\phi}_2(\phi_B - \bar{\phi}_B)\phi_3^s + \phi_B((\phi_4 - 2\phi_3^s)\bar{\phi}_3^a + 2\phi_3^s\bar{\phi}_3^s + \phi_4(\bar{\phi}_3^s + \bar{\phi}_4)) - \phi_4(\bar{\phi}_3^a + \bar{\phi}_3^s)\bar{\phi}_B)(x'_2 + x'_3))f^+ \\
& + \bar{r}(2\bar{\phi}_2(\phi_B - \bar{\phi}_B)\phi_3^s + \phi_B((\phi_4 - 2\phi_3^s)\bar{\phi}_3^a + 2\phi_3^s\bar{\phi}_3^s + \phi_4(\bar{\phi}_3^s + \bar{\phi}_4)) - \phi_4(\bar{\phi}_3^a + \bar{\phi}_3^s)\bar{\phi}_B)(x'_2 + x'_3)). \tag{A2}
\end{aligned}$$

For the S -wave expressions of Fig. 2 (c7):

$$\begin{aligned}
H_{E_{c7}}^{LL,S}(x, x', y) = & \frac{M^3}{f^- - f^+} ((\bar{r} + (r - \bar{r})f^+)(\phi_B(2\phi_3^a\bar{\phi}_3^a + 2\phi_3^s\bar{\phi}_3^s + \phi_2\bar{\phi}_2 + 2\phi_4\bar{\phi}_2 + \phi_4\bar{\phi}_4) \\
& - (2\phi_3^a\bar{\phi}_3^a + 2\phi_3^s\bar{\phi}_3^s + \phi_2\bar{\phi}_2 + \phi_4\bar{\phi}_4)\bar{\phi}_B)x'_2x'_3f^{-2} + (-(r - \bar{r})x_2x_3(\phi_B(2\phi_3^a\bar{\phi}_3^a + 2\phi_3^s\bar{\phi}_3^s
\end{aligned}$$

TABLE VII: The expressions of a^{LL} and a^{SP} for the W -emission and W -exchange diagrams.

R_{ij}	a^{LL}	a^{SP}
$C_{a1,a2,a4,a5,b1,b4,c1,c3,d1,d3,e1,f1}$	$V_{cb}V_{cq}^*(C_2 - C_1) - V_{tb}V_{tq}^*(C_4 - C_3 + C_{10} - C_9)$	$-V_{tb}V_{tq}^*(C_6 - C_5 + C_8 - C_7)$
$C_{a3,b2,c2,f2}$	$V_{cb}V_{cq}^*(2C_1 + C_2) - V_{tb}V_{tq}^*(2C_3 + C_4 + 2C_9 + C_{10})$	$-V_{tb}V_{tq}^*(2C_5 + C_6 + 2C_7 + C_8)$
$C_{a6,b6,c5,d5,f3}$	$V_{cb}V_{cq}^*2(C_1 - C_2) - V_{tb}V_{tq}^*2(C_3 - C_4 + C_9 - C_{10})$	$-V_{tb}V_{tq}^*2(C_5 - C_6 + C_7 - C_8)$
$C_{a7,b7,c6,f4}$	$V_{cb}V_{cq}^*(-C_1 - 2C_2) - V_{tb}V_{tq}^*(-C_3 - 2C_4 - C_9 - 2C_{10})$	$-V_{tb}V_{tq}^*(-C_5 - 2C_6 - C_7 - 2C_8)$
$C_{b3,d2,e2}$	$V_{cb}V_{cq}^*(-\frac{1}{4}C_1 + C_2) - V_{tb}V_{tq}^*(-\frac{1}{4}C_3 + C_4 - \frac{1}{4}C_9 + C_{10})$	$-V_{tb}V_{tq}^*(-\frac{1}{4}C_5 + C_6 - \frac{1}{4}C_7 + C_8)$
C_{b5}	$V_{cb}V_{cq}^*(\frac{5}{4}C_1 + C_2) - V_{tb}V_{tq}^*(\frac{5}{4}C_3 + C_4 + \frac{5}{4}C_9 + C_{10})$	$-V_{tb}V_{tq}^*(\frac{5}{4}C_5 + C_6 + \frac{5}{4}C_7 + C_8)$
C_{c4}	$V_{cb}V_{cq}^*(-C_1 - \frac{5}{4}C_2) - V_{tb}V_{tq}^*(-C_3 - \frac{5}{4}C_4 - C_9 - \frac{5}{4}C_{10})$	$-V_{tb}V_{tq}^*(-C_5 - \frac{5}{4}C_6 - C_7 - \frac{5}{4}C_8)$
$C_{c7,d7,e4}$	$V_{cb}V_{cq}^*(\frac{1}{4}C_2 - C_1) - V_{tb}V_{tq}^*(\frac{1}{4}C_4 - C_3 + \frac{1}{4}C_{10} - C_9)$	$-V_{tb}V_{tq}^*(\frac{1}{4}C_6 - C_5 + \frac{1}{4}C_8 - C_7)$
C_{d4}	$V_{cb}V_{cq}^*\frac{5}{4}(C_1 - C_2) - V_{tb}V_{tq}^*\frac{5}{4}(C_3 - C_4 + C_9 - C_{10})$	$-V_{tb}V_{tq}^*\frac{5}{4}(C_5 - C_6 + C_7 - C_8)$
C_{d6}	$V_{cb}V_{cq}^*4(C_2 - C_1) - V_{tb}V_{tq}^*4(C_4 - C_3 + C_{10} - C_9)$	$-V_{tb}V_{tq}^*4(C_6 - C_5 + C_8 - C_7)$
C_{e3}	$V_{cb}V_{cq}^*(C_2 - C_1)/4 - V_{tb}V_{tq}^*(C_4 - C_3 + C_{10} - C_9)/4$	$-V_{tb}V_{tq}^*(C_6 - C_5 + C_8 - C_7)/4$
C_{g1}	0	0
C_{g2}	$V_{cb}V_{cq}^*\frac{9}{4}(-C_1) - V_{tb}V_{tq}^*\frac{9}{4}(-C_3 - C_9)$	$-V_{tb}V_{tq}^*\frac{9}{4}(-C_5 - C_7)$
C_{g3}	$V_{cb}V_{cq}^*\frac{9}{4}(C_2 - C_1) - V_{tb}V_{tq}^*\frac{9}{4}(C_4 - C_3 + C_{10} - C_9)$	$-V_{tb}V_{tq}^*\frac{9}{4}(C_6 - C_5 + C_8 - C_7)$
C_{g4}	$V_{cb}V_{cq}^*\frac{9}{4}C_2 - V_{tb}V_{tq}^*\frac{9}{4}(C_4 + C_{10})$	$-V_{tb}V_{tq}^*\frac{9}{4}(C_6 + C_8)$
$E_{a1,a2,a3,a5,b1,b2,b4}$	$V_{cb}V_{cq}^*(3C_1 + C_2) - V_{tb}V_{tq}^*(3C_3 + C_4 + 3C_9 + C_{10})$	$-V_{tb}V_{tq}^*(3C_5 + C_6 + 3C_7 + C_8)$
$E_{a6,a7,b6,b7,c1,c2,d1,d2}$	$V_{cb}V_{cq}^*C_2 - V_{tb}V_{tq}^*(C_4 + C_{10})$	$-V_{tb}V_{tq}^*(C_6 + C_8)$
$E_{c5,c7,d6}$	$V_{cb}V_{cq}^*(C_2 + \frac{3}{4}C_1) - V_{tb}V_{tq}^*(C_4 - \frac{3}{4}C_3 + C_{10} - \frac{3}{4}C_9)$	$-V_{tb}V_{tq}^*(C_6 - \frac{3}{4}C_8 + C_8 - \frac{3}{4}C_7)$

TABLE IX: The virtualities of the internal propagators $t_{A,B,C,D}$ for the W -emission and W -exchange diagrams.

R_{ij}	$\frac{t_A}{M^2}$	$\frac{t_B}{M^2}$	$\frac{t_C}{M^2}$	$\frac{t_D}{M^2}$
C_{a1}	f^+x_1y	$f^+(f^- - 1)x_2x'_2$	$f^+(f^- - y)(x_2 - 1) + r_c^2$	$f^+(f^-(x'_2 - 1) - x'_2 + y) + r_c^2$
C_{a2}	f^+x_1y	$f^+(f^- - 1)x_2x'_2$	$f^+(x_1 - 1)(f^-(1 - x'_2) + x'_2) + r_c^2$	$f^+(f^-(x'_2 - 1) - x'_2 + y) + r_c^2$
C_{a3}	f^+x_1y	$f^+(f^- - 1)x_2x'_2$	$f^+x_1((f^- - 1)x'_3 + y)$	$f^+(x_1 - 1)(f^-(1 - x'_2) + x'_2) + r_c^2$
C_{a4}	f^+x_1y	$f^+(x_1 + x_2)((f^- - 1)x'_2 + y)$	$f^+y(x_1 + x_2)$	$r_c^2 + f^+(f^-(x'_2 - 1) - x'_2 + y)$
C_{a5}	f^+x_1y	$f^+(x_1 + x_2)((f^- - 1)x'_2 + y)$	$f^+x_1((f^- - 1)x'_2 + y)$	$f^+(f^-(x'_2 - 1) - x'_2 + y) + r_c^2$
C_{a6}	f^+x_1y	$f^+(f^- - 1)x_2x'_2$	f^+x_1	$f^+(x_1 - 1)(f^-(1 - x'_2) + x'_2) + r_c^2$
C_{a7}	f^+x_1y	$f^+(f^- - 1)x_2x'_2$	$(f^+(x_1 - 1) + 1)((f^- - 1)x'_1 + y) + r_c^2$	$f^+(x_1 - 1)(f^-(1 - x'_2) + x'_2) + r_c^2$
C_{b1}	f^+x_1y	$f^+(f^- - 1)x_2x'_2$	$f^+(x_2 - 1)(f^- - y) + r_c^2$	$f^+(f^- - 1)x_2(x'_2 + x'_3)$
C_{b2}	f^+x_1y	$f^+(f^- - 1)x_2x'_2$	$f^+(x_1 + x_2)((f^- - 1)(x'_2 + x'_3) + y)$	$f^+(f^- - 1)x_2(x'_2 + x'_3)$
C_{b3}	f^+x_1y	$f^+(f^- - 1)x_2x'_2$	$f^+x_1((f^- - 1)x'_3 + y)$	$f^+(x_1 + x_2)((f^- - 1)(x'_2 + x'_3) + y)$
C_{b4}	f^+x_1y	$f^+(x_1 + x_2)((f^- - 1)x'_2 + y)$	$f^+y(x_1 + x_2)$	$f^+(x_1 + x_2)((f^- - 1)(x'_2 + x'_3) + y)$
C_{b5}	f^+x_1y	$f^+(x_1 + x_2)((f^- - 1)x'_2 + y)$	$f^+x_1((f^- - 1)x'_2 + y)$	$f^+(x_1 + x_2)((f^- - 1)(x'_2 + x'_3) + y)$
C_{b6}	f^+x_1y	$(f^- - 1)f^+x_2x'_2$	f^+x_1	$(f^- - 1)f^+x_2(x'_2 + x'_3)$
C_{b7}	f^+x_1y	$(f^- - 1)f^+x_2x'_2$	$(f^+(x_1 - 1) + 1)((f^- - 1)x'_1 + y) + r_c^2$	$(f^- - 1)f^+x_2(x'_2 + x'_3)$
C_{c1}	f^+x_1y	$(f^- - 1)f^+x_2x'_2$	$f^+(x_2 - 1)(f^- - y) + r_c^2$	$-f^-(x'_3 - 1)(f^+(x_2 - 1) + 1)$ $+f^+(x_2 - 1)(x'_3 - 1) + r_c^2 + x'_3 - 1$ $-f^-(x'_3 - 1)(f^+(x_2 - 1) + 1)$ $+f^+(x_2 - 1)(x'_3 - 1) + r_c^2 + x'_3 - 1$
C_{c2}	f^+x_1y	$(f^- - 1)f^+x_2x'_2$	$f^+x_1((f^- - 1)x'_3 + y)$	$-f^-(x'_3 - 1)(f^+(x_2 - 1) + 1)$ $+f^+(x_2 - 1)(x'_3 - 1) + r_c^2 + x'_3 - 1$ $-f^-(x'_3 - 1)(f^+(x_2 - 1) + 1)$ $+f^+(x_2 - 1)(x'_3 - 1) + r_c^2 + x'_3 - 1$
C_{c3}	f^+x_1y	$f^+(x_1 + x_2)((f^- - 1)x'_2 + y)$	$f^+y(x_1 + x_2)$	$(f^+x_3 - 1)[f^-(x'_3 - 1) - (x'_3 + y - 1)] + r_c^2$
C_{c4}	f^+x_1y	$f^+(x_1 + x_2)((f^- - 1)x'_2 + y)$	$f^+x_1(y + (f^- - 1)x'_2)$	$(f^+x_3 - 1)[f^-(x'_3 - 1) - (x'_3 + y - 1)] + r_c^2$
C_{c5}	f^+x_1y	$(f^- - 1)f^+x_2x'_2$	f^+x_1	$-f^-(x'_3 - 1)(f^+(x_2 - 1) + 1)$ $+f^+(x_2 - 1)(x'_3 - 1) + r_c^2 + x'_3 - 1$
C_{c6}	f^+x_1y	$(f^- - 1)f^+x_2x'_2$	$f^-(x'_3 - 1)(f^+x_3 - 1)$ $-(f^+x_3 - 1)(x'_3 + y - 1) + r_c^2$	$-f^-(x'_3 - 1)(f^+(x_2 - 1) + 1)$ $+f^+(x_2 - 1)(x'_3 - 1) + r_c^2 + x'_3 - 1$
C_{c7}	f^+x_1y	$(f^- - 1)f^+x_2x'_2$	$(f^+(x_1 - 1) + 1)((f^- - 1)x'_1 + y) + r_c^2$	$(f^+x_3 - 1)[f^-(x'_3 - 1) - (x'_3 + y - 1)] + r_c^2$
C_{d1}	f^+x_1y	$(f^- - 1)f^+x_2x'_2$	$f^+(x_2 - 1)(f^- - y) + r_c^2$	$f^+x_2((f^- - 1)x'_2 - y + 1) - f^+x'_2 + x'_2 + y$
C_{d2}	f^+x_1y	$(f^- - 1)f^+x_2x'_2$	$f^+x_1((f^- - 1)x'_3 + y)$	$f^+x_2((f^- - 1)x'_2 - y + 1) - f^+x'_2 + x'_2 + y$
C_{d3}	f^+x_1y	$f^+(x_1 + x_2)((f^- - 1)x'_2 + y)$	$f^+y(x_1 + x_2)$	$-f^+(x_3 - 1)((f^- - 1)x'_2 + 1) - f^+x'_2 + x'_2$
C_{d4}	f^+x_1y	$f^+(x_1 + x_2)((f^- - 1)x'_2 + y)$	$f^+x_1(y + (f^- - 1)x'_2)$	$-f^+(x_3 - 1)((f^- - 1)x'_2 + 1) - f^+x'_2 + x'_2$
C_{d5}	f^+x_1y	$(f^- - 1)f^+x_2x'_2$	f^+x_1	$-f^+(x_3 - 1)((f^- - 1)x'_2 + 1) - f^+x'_2 + x'_2$
C_{d6}	f^+x_1y	$(f^- - 1)f^+x_2x'_2$	$f^+((f^- - 1)x'_2 + 1)(x_1 + x_2) - f^+x'_2 + x'_2$	$f^+x_2((f^- - 1)x'_2 - y + 1) - f^+x'_2 + x'_2 + y$
C_{d7}	f^+x_1y	$(f^- - 1)f^+x_2x'_2$	$(f^+(x_1 - 1) + 1)((f^- - 1)x'_1 + y) + r_c^2$	$f^+x_2((f^- - 1)x'_2 - y + 1) - f^+x'_2 + x'_2 + y$
C_{e1}	$f^+(f^- - 1)x_2x'_2$	$f^+(1 - x_3)((f^- - 1)x'_2 + y)$	$f^+x_2((f^- - 1)x'_2 + y)$	$f^+(f^-(x'_2 - 1) - x'_2 + y) + r_c^2$
C_{e2}	$f^+(f^- - 1)x_2x'_2$	$f^+(1 - x_3)((f^- - 1)x'_2 + y)$	$f^+x_2((f^- - 1)x'_2 + y)$	$f^+(x_1 + x_2)((f^- - 1)(x'_2 + x'_3) + y)$
C_{e3}	$f^+(f^- - 1)x_2x'_2$	$f^+(1 - x_3)((f^- - 1)x'_2 + y)$	$f^+x_2((f^- - 1)x'_2 + y)$	$f^+((f^- - 1)x'_2 + 1)(x_1 + x_2) - f^+x_2p + x'_2$
C_{e4}	$f^+(f^- - 1)x_2x'_2$	$f^+(1 - x_3)((f^- - 1)x'_2 + y)$	$f^+x_2((f^- - 1)x'_2 + y)$	$(f^+x_3 - 1)[f^-(x'_3 - 1) - (x'_3 + y - 1)] + r_c^2$
C_{f1}	$f^+(f^- - 1)x_2x'_2$	$f^+(1 - x_3)((f^- - 1)x'_2 + y)$	$(f^- - 1)f^+x'_2(x_1 + x_2)$	$r_c^2 + f^+(f^-(x'_2 - 1) - x'_2 + y)$
C_{f2}	$f^+(f^- - 1)x_2x'_2$	$f^+(1 - x_3)((f^- - 1)x'_2 + y)$	$(f^- - 1)f^+x'_2(x_1 + x_2)$	$f^+(-(x_3 - 1))((f^- - 1)(x'_2 + x'_3) + y)$
C_{f3}	$f^+(f^- - 1)x_2x'_2$	$f^+(1 - x_3)((f^- - 1)x'_2 + y)$	$(f^- - 1)f^+x'_2(x_1 + x_2)$	$-f^+(x_3 - 1)((f^- - 1)x'_2 + 1) - f^+x'_2 + x'_2$
C_{f4}	$f^+(f^- - 1)x_2x'_2$	$f^+(1 - x_3)((f^- - 1)x'_2 + y)$	$(f^- - 1)f^+x'_2(x_1 + x_2)$	$(f^+x_3 - 1)[f^-(x'_3 - 1) - (x'_3 + y - 1)] + r_c^2$
C_{g2}	f^+x_1y	$(f^- - 1)f^+x_2x'_2$	$f^+(x_1 + x_2)((f^- - 1)x'_2 + y)$	$f^+(x_1 + x_2)((f^- - 1)(x'_2 + x'_3) + y)$
C_{g3}	f^+x_1y	$(f^- - 1)f^+x_2x'_2$	$f^+(x_1 + x_2)((f^- - 1)x'_2 + y)$	$f^+((f^- - 1)x'_2 + 1)(x_1 + x_2) - f^+x'_2 + x'_2$
C_{g4}	f^+x_1y	$(f^- - 1)f^+x_2x'_2$	$f^+(x_1 + x_2)((f^- - 1)x'_2 + y)$	$(f^+x_3 - 1)[f^-(x'_3 - 1) - (x'_3 + y - 1)] + r_c^2$
E_{a1}	$(f^- - 1)f^+x_3x'_3$	$(f^- - 1)f^+(1 - x_1)(1 - x'_1)$	$(f^- - 1)f^+x'_3(1 - x_1)$	$r_c^2 + f^+(x'_1 - 1 - f^-x'_1)$
E_{a2}	$(f^- - 1)f^+x_3x'_3$	$(f^- - 1)f^+(1 - x_1)(1 - x'_1)$	$(f^- - 1)f^+x'_3(1 - x'_1)$	$r_c^2 + f^+(x'_1 - 1 - f^-x'_1)$
E_{a3}	$(f^- - 1)f^+x_3x'_3$	$(f^- - 1)f^+x_2x'_2$	$r_c^2 + f^+(x_2 - 1)(f^- + x_3 - f^-x'_3)$	$r_c^2 + f^+(x'_1 - 1 - f^-x'_1)$
E_{a5}	$(f^- - 1)f^+x_3x'_3$	$(f^- - 1)f^+x_2x'_2$	$r_c^2 - 1 + x'_2 - f^-(x'_2 - 1)$ $(1 + f^+(x_3 - 1)) + f^+(x'_2 - 1)(x_3 - 1)$	$r_c^2 - f^+(x_3 - 1)(f^-(x'_2 - 1) - x'_2)$
E_{a6}	$(f^- - 1)f^+x_3x'_3$	$(f^- - 1)f^+x_2x'_2$	$f^+x_3((f^- - 1)x'_3 + y)$	$r_c^2 - f^+(x_3 - 1)(f^-(x'_2 - 1) - x'_2)$
E_{a7}	$(f^- - 1)f^+x_3x'_3$	$(f^- - 1)f^+x_2x'_2$	$f^+x_3((f^- - 1)x'_3 - y + 1) + x'_3(1 - f^-) + y$	$r_c^2 - f^+(x_3 - 1)(f^-(x'_2 - 1) - x'_2)$
E_{b1}	$(f^- - 1)f^+x_3x'_3$	$(f^- - 1)f^+(1 - x_1)(1 - x'_1)$	$(f^- - 1)f^+(1 - x_1)x'_3$	$f^- - 1 + r_c^2 + f^+x_1 - f^-f^+x_1$
E_{b2}	$(f^- - 1)f^+x_3x'_3$	$(f^- - 1)f^+(1 - x_1)(1 - x'_1)$	$(f^- - 1)f^+x_3(1 - x'_1)$	$r_c^2 + f^- - 1 + f^+x_1 - f^-f^+x_1$
E_{b4}	$(f^- - 1)f^+x_3x'_3$	$(f^- - 1)f^+x_2x'_2$	$r_c^2 + f^- - 1 + f^+x_1 - f^-f^+x_1$	$r_c^2 - 1 - f^-(1 + f^+(x_2 - 1))$ $(x'_3 - 1) + f^+(x_2 - 1)(x'_3 - 1) + x'_3$
E_{b6}	$(f^- - 1)f^+x_3x'_3$	$(f^- - 1)f^+x_2x'_2$	$f^+x_3((f^- - 1)x'_3 + y)$	$r_c^2 - 1 - f^-(1 + f^+(x_2 - 1))$ $(x'_3 - 1) + f^+(x_2 - 1)(x'_3 - 1) + x'_3$
E_{b7}	$(f^- - 1)f^+x_3x'_3$	$(f^- - 1)f^+x_2x'_2$	$x'_3 - f^-x'_3 + f^+x_3(1 + (f^- - 1)x'_3 - y) + y$	$r_c^2 - 1 - f^-(1 + f^+(x_2 - 1))$ $(x'_3 - 1) + f^+(x_2 - 1)(x'_3 - 1) + x'_3$
E_{c1}	$(f^- - 1)f^+x_3x'_3$	$(f^- - 1)f^+(1 - x_1)(1 - x'_1)$	$f^+x'_3(f^- - 1 + x_1 - f^-x_1)$	$f^+(1 - x_1)((f^- - 1)(1 - x'_1) + y)$
E_{c2}	$(f^- - 1)f^+x_3x'_3$	$(f^- - 1)f^+(1 - x_1)(1 - x'_1)$	$(f^- - 1)f^+x_3(1 - x'_1)$	$f^+(1 - x_1)((f^- - 1)(1 - x'_1) + y)$
E_{c5}	$(f^- - 1)f^+x_3x'_3$	$(f^- - 1)f^+x_2x'_2$	$f^+x_3((f^- - 1)x'_3 + y)$	$f^+(1 - x_1)((f^- - 1)(1 - x'_1) + y)$
E_{c7}	$(f^- - 1)f^+x_3x'_3$	$(f^- - 1)f^+x_2x'_2$	$f^+x_3(1 + (f^- - 1)x'_3 - y) + x'_3 - f^-x'_3 + y$	$f^+x_2((f^- - 1)x'_2 + y)$
E_{d1}	$(f^- - 1)f^+x_3x'_3$	$(f^- - 1)f^+(1 - x_1)(1 - x'_1)$	$f^+(f^- - 1 + x_1 - f^-x_1)x'_3$	$y - (f^- - 1)(x'_2 + x'_3) + f^+(x_2 + x_3)$ $((f^- - 1)x'_2 + (f^- - 1)x'_3 - y + 1)$
E_{d2}	$(f^- - 1)f^+x_3x'_3$	$(f^- - 1)f^+(1 - x_1)(1 - x'_1)$	$(f^- - 1)f^+x_3(1 - x'_1)$	$y - (f^- - 1)(x'_2 + x'_3) + f^+(x_2 + x_3)$ $((f^- - 1)x'_2 + (f^- - 1)x'_3 - y + 1)$

-
- [1] Belle collaboration, Observation of $B^\pm \rightarrow p\bar{p}K^\pm$, Phys. Rev. Lett. **88** (2002) 181803 [hep-ex/0202017].
- [2] Belle collaboration, Observation of $B^+ \rightarrow p\bar{p}\pi^+$, $B^0 \rightarrow p\bar{p}K^0$, and $B^+ \rightarrow p\bar{p}K^{*+}$, Phys. Rev. Lett. **92** (2004) 131801 [hep-ex/0310018].
- [3] R. Chistov, Baryonic B Decays, J. Phys. Conf. Ser. **675** (2016) 022007.
- [4] Belle collaboration, Study of $B^+ \rightarrow p\bar{p}K^+$ and $B^+ \rightarrow p\bar{p}\pi^+$, Phys. Lett. B **659** (2008) 80 [arXiv: 0706.4167].
- [5] Belle collaboration, Study of the baryon-antibaryon low-mass enhancements in charmless three-body baryonic B decays, Phys. Lett. B **617** (2005) 141 [hep-ex/0503047].
- [6] M. Suzuki, Partial waves of baryon-antibaryon in three-body B meson decay, J. Phys. G **34** (2007) 283 [hep-ph/0609133].
- [7] H. Y. Cheng, Exclusive baryonic B decays Circa 2005, Int. J. Mod. Phys. A **21** (2006) 4209 [hep-ph/0603003].
- [8] BaBar and Belle collaborations, The Physics of the B Factories, Eur. Phys. J. C **74** (2014) 3026 [arXiv: 1406.6311].
- [9] J. Barnard, T. Gherghetta, A. Medina and T. S. Ray, Radiative corrections to the composite Higgs mass from a gluon partner, JHEP **10** (2013) 055 [arXiv: 1307.4778].
- [10] LHCb collaboration, Evidence for CP Violation in $B^+ \rightarrow p\bar{p}K^+$ Decays, Phys. Rev. Lett. **113** (2014) 141801 [arXiv: 1407.5907].
- [11] X. Huang, Y. K. Hsiao, J. Wang and L. Sun, Baryonic B Meson Decays, Adv. High Energy Phys. **2022** (2022) 4343824 [arXiv: 2109.02897].
- [12] H. Y. Cheng, Status of baryonic B decays, Nucl. Phys. B Proc. Suppl. **163** (2007) 68 [hep-ph/0607061].
- [13] J. L. Rosner, Low mass baryon anti-baryon enhancements in B decays, Phys. Rev. D **68** (2003) 014004 [hep-ph/0303079].
- [14] W. S. Hou and A. Soni, Pathways to rare baryonic B decays, Phys. Rev. Lett. **86** (2001) 4247 [hep-ph/0008079].
- [15] Belle collaboration, Observation of $\bar{B}^0 \rightarrow \Lambda_c^+ \bar{p}$ decay, Phys. Rev. Lett. **90** (2003) 121802 [hep-ex/0212052].
- [16] Belle collaboration, Observation of $B^+ \rightarrow \Xi_c^0 \Lambda_c^+$ and evidence for $B^0 \rightarrow \Xi_c^- \Lambda_c^+$, Phys. Rev. D **74** (2006) 111105 [hep-ex/0510074].
- [17] Particle Data collaboration, Review of Particle Physics, Phys. Rev. D **110** (2024) 030001.
- [18] V. L. Chernyak and I. R. Zhitnitsky, B meson exclusive decays into baryons, Nucl. Phys. B **345** (1990) 137.
- [19] P. Ball and H. G. Dosch, Branching ratios of exclusive decays of bottom mesons into baryon - anti-baryon pairs, Z. Phys. C **51** 445 (1991).
- [20] A. Datta and P. J. O'Donnell, A New state of baryonium, Phys. Lett. B **567** (2003) 273 [hep-ph/0306097].
- [21] Belle collaboration, First Measurements of Absolute Branching Fractions of the Ξ_c^0 Baryon at Belle, Phys. Rev. Lett. **122** (2019) 082001 [arXiv: 1811.09738].
- [22] Belle collaboration, First measurements of absolute branching fractions of the Ξ_c^+ baryon at Belle, Phys. Rev. D **100** (2019) 031101 [arXiv: 1904.12093].
- [23] LHCb collaboration, Study of beauty hadron decays into pairs of charm hadrons, Phys. Rev. Lett. **112**, 202001 (2014) [arXiv: 1403.3606].
- [24] Belle collaboration, Measurements of the Branching Fractions $\mathcal{B}(B^- \rightarrow \bar{\Lambda}_c^- \Xi_c^{\prime 0})$, $\mathcal{B}(B^- \rightarrow \bar{\Lambda}_c^- \Xi_c(2645)^0)$ and $\mathcal{B}(B^- \rightarrow \bar{\Lambda}_c^- \Xi_c(2790)^0)$, Phys. Rev. D **100** (2019) 112010 [arXiv: 1911.12530].
- [25] H. Y. Cheng, C. K. Chua and S. Y. Tsai, Doubly charmful baryonic B decays, Phys. Rev. D **73** (2006) 074015 [hep-ph/0512335].
- [26] H. Y. Cheng, C. K. Chua and Y. K. Hsiao, Study of $\bar{B} \rightarrow \Lambda_c \bar{\Lambda}_c$ and $\bar{B} \rightarrow \Lambda_c \bar{\Lambda}_c \bar{K}$, Phys. Rev. D **79**, 114004 (2009) [arXiv: 0902.4295].
- [27] C. H. Chen, Production of doubly charmed baryons in B decays, Phys. Lett. B **638** (2006) 214 [hep-ph/0603070].
- [28] Y. K. Hsiao, Study of two-body doubly charmful baryonic B decays with $SU(3)$ flavor symmetry, JHEP **11**, 117 (2023) [arXiv: 2309.16919].
- [29] T. Kurimoto, H. n. Li, and A. I. Sanda, Leading power contributions to $B \rightarrow \pi, \rho$ transition form-factors, Phys. Rev. D **65** (2001) 014007 [hep-ph/0105003].
- [30] C. D. Lu and M. Z. Yang, B to light meson transition form-factors calculated in perturbative QCD approach, Eur. Phys. J. C **28** (2003) 515 [hep-ph/0212373].
- [31] A. Ali, G. Kramer, Y. Li, C. D. Lu, Y. L. Shen, W. Wang, and Y. M. Wang, Charmless non-leptonic B_s decays to PP , PV and VV final states in the pQCD approach, Phys. Rev. D **76** (2007) 074018 [hep-ph/0703162].
- [32] W. Wang, B to tensor meson form factors in the perturbative QCD approach, Phys. Rev. D **83** (2011) 014008 [arXiv: 1008.5326].
- [33] Z. Rui, Y. Li, and H. n. Li, Four-body decays $B_{(s)} \rightarrow (K\pi)_{S/P}(K\pi)_{S/P}$ in the perturbative QCD approach, JHEP **05** (2021) 082 [arXiv:2103.00642].
- [34] J. Chai, S. Cheng, Y. h. Ju, D. C. Yan, C. D. Lü, and Z. J. Xiao, Charmless two-body B meson decays in the perturbative QCD factorization approach, Chin. Phys. C **46** (2022) 123103 [arXiv: 2207.04190].
- [35] C. H. Chou, H. H. Shih, S. C. Lee, and H. n. Li, $\Lambda_b \rightarrow \Lambda J/\psi$ decay in perturbative QCD, Phys. Rev. D **65** (2002) 074030 [hep-ph/0112145].
- [36] H. H. Shih, S. C. Lee, and H. n. Li, The $\Lambda_b \rightarrow p l \bar{\nu}$ decay in perturbative QCD, Phys. Rev. D **59** (1999) 094014 [hep-ph/9810515].
- [37] H. H. Shih, S. C. Lee, and H. n. Li, Applicability of perturbative QCD to $\Lambda_b \rightarrow \Lambda_c$ decays, Phys. Rev. D **61** (2000) 114002 [hep-ph/9906370].
- [38] H. H. Shih, S. C. Lee, and H. n. Li, Asymmetry parameter in the polarized $\Lambda_b \rightarrow \Lambda_c l \bar{\nu}$ decay, Chin. J. Phys. **39**, 328

- (2001).
- [39] X. G. He, T. Li, X. Q. Li, and Y. M. Wang, PQCD calculation for $\Lambda_b \rightarrow \Lambda\gamma$ in the standard model, Phys. Rev. D **74** (2006) 034026 [hep-ph/0606025].
 - [40] C. D. Lu, Y. M. Wang, H. Zou, A. Ali, and G. Kramer, Anatomy of the pQCD approach to the baryonic decays $\Lambda_b \rightarrow p\pi, pK$, Phys. Rev. D **80** (2009) 034011 [arXiv: 0906.1479].
 - [41] J. J. Han, Y. Li, H. n. Li, Y. L. Shen, Z. J. Xiao, and F. S. Yu, $\Lambda_b \rightarrow p$ transition form factors in perturbative QCD, Eur. Phys. J. C **82** (2022) 686 [arXiv: 2202.04804].
 - [42] C. Q. Zhang, J. M. Li, M. K. Jia, and Z. Rui, Nonleptonic two-body decays of $\Lambda_b \rightarrow \Lambda_c\pi, \Lambda_c K$ in the perturbative QCD approach, Phys. Rev. D **105** (2022) 073005 [arXiv: 2202.09181].
 - [43] Z. Rui, C. Q. Zhang, J. M. Li and M. K. Jia, Investigating the color-suppressed decays $\Lambda_b \rightarrow \Lambda\psi$ in the perturbative QCD approach, Phys. Rev. D **106** (2022) 053005 [arXiv: 2206.04501].
 - [44] Z. Rui, J. M. Li and C. Q. Zhang, Estimates of exchange topological contributions and CP -violating observables in $\Lambda_b \rightarrow \Lambda\phi$ decay, Phys. Rev. D **107** (2023) 053009 [arXiv: 2210.15357].
 - [45] Z. Rui, J. M. Li and C. Q. Zhang, Mixing effects of $\eta - \eta'$ in $\Lambda_b \rightarrow \Lambda\eta^{(\prime)}$ decays, Phys. Rev. D **107** (2023) 093008 [arXiv: 2302.13785].
 - [46] Z. Rui, J. M. Li and C. Q. Zhang, Estimates on the isospin-violating $\Lambda_b \rightarrow \Sigma^0\phi, \Sigma^0 J/\psi$ decays and the $\Sigma - \Lambda$ mixing, Phys. Rev. D **108** (2023) 033004 [arXiv: 2308.02262].
 - [47] Z. Rui and Z. T. Zou, Charmonium decays of beauty baryons in the perturbative QCD approach, Phys. Rev. D **109** (2024) 033013 [arXiv: 2310.19031].
 - [48] J. X. Yu, J. J. Han, Y. Li, H. n. Li, Z. J. Xiao and F. S. Yu, Establishing CP violation in b -baryon decays, [arXiv:2409.02821].
 - [49] X. G. He, T. Li, X. Q. Li and Y. M. Wang, Calculation of $BR(\bar{B}^0 \rightarrow \Lambda_c^+ + \bar{p})$ in the PQCD approach, Phys. Rev. D **75** (2007) 034011 [hep-ph/0607178].
 - [50] R. H. Li, X. X. Wang, A. I. Sanda and C. D. Lu, Decays of B meson to two charmed mesons, Phys. Rev. D **81** (2010) 034006 [arXiv: 0910.1424].
 - [51] Z. Rui, Z. Zhitian and C. D. Lu, The Double charm decays of B_c Meson in the Perturbative QCD Approach, Phys. Rev. D **86** (2012) 074019 [arXiv: 1203.2303].
 - [52] P. Ball, V. M. Braun, and E. Gardi, Distribution amplitudes of the Λ_b baryon in QCD, Phys. Lett. B **665** (2008) 197 [arXiv: 0804.2424].
 - [53] A. Ali, C. Hambrock, and A. Y. Parkhomenko, Light-cone wave functions of heavy baryons, Theor. Math. Phys. **170** (2012) 2.
 - [54] A. Ali, C. Hambrock, A. Y. Parkhomenko, and W. Wang, Light-Cone distribution amplitudes of the ground state bottom baryons in HQET, Eur. Phys. J. C **73** (2013) 2302 [arXiv: 1212.3280].
 - [55] V. M. Braun, S. E. Derkachov, and A. N. Manashov, Integrability of the evolution equations for heavy-light baryon distribution amplitudes, Phys. Lett. B **738** (2014) 334 [arXiv: 1406.0664].
 - [56] Y. M. Wang and Y. L. Shen, Perturbative corrections to $\Lambda_b \rightarrow \Lambda$ form factors from QCD Light-Cone Sum Rules, JHEP **02** (2016) 179 [arXiv: 1511.09036].
 - [57] G. Bell, T. Feldmann, Y. M. Wang, and M. W. Y. Yip, Light-cone distribution amplitudes for heavy-quark hadrons, JHEP **11** (2013) 191 [arXiv: 1308.6114].
 - [58] Y. M. Wang, Y. L. Shen, and C. D. Lu, $\Lambda_b \rightarrow p, \Lambda$ transition form factors from QCD light-cone sum rules, Phys. Rev. D **80** (2009) 074012 [arXiv: 0907.4008].
 - [59] Z. G. Wang, Analysis of the $\frac{1}{2}^\pm$ antitriplet heavy baryon states with QCD sum rules, Eur. Phys. J. C **68** (2010) 479 [arXiv: 1001.1652].
 - [60] M. Beneke, G. Buchalla, M. Neubert and C. T. Sachrajda, QCD factorization for exclusive, nonleptonic B meson decays: General arguments and the case of heavy light final states, Nucl. Phys. B **591** (2000) 313 [hep-ph/0006124].
 - [61] A. G. Grozin and M. Neubert, Asymptotics of heavy meson form-factors, Phys. Rev. D **55** (1997) 272 [hep-ph/9607366].
 - [62] T. Kurimoto, Uncertainty in the leading order PQCD calculations of B meson decays, Phys. Rev. D **74** (2006) 014027 [hep-ph/0605112].
 - [63] Y. Yang, L. Lang, X. Zhao, J. Huang and J. Sun, Reinvestigating the $B \rightarrow PP$ decays by including the contributions from ϕ_{B2} , Phys. Rev. D **103** (2021) 056006 [arXiv: 2012.10581].
 - [64] Y. Yang, X. Zhao, L. Lang, J. Huang and J. Sun, Reinvestigating $B \rightarrow PV$ decays by including contributions from ϕ_{B2} with the perturbative QCD approach, Chin. Phys. C **46** (2022) 083103 [arXiv: 2201.12834].
 - [65] J. Hua, H. n. Li, C. D. Lu, W. Wang and Z. P. Xing, Global analysis of hadronic two-body B decays in the perturbative QCD approach, Phys. Rev. D **104** (2021) 016025 [arXiv: 2012.15074].
 - [66] W. Wang, Y. M. Wang, J. Xu, and S. Zhao, B -meson light-cone distribution amplitude from the Euclidean quantities, Phys. Rev. D **102** (2020) 011502(R) [arXiv: 1908.09933].
 - [67] H. n. Li and H. S. Liao, B meson wave function in k_T factorization, Phys. Rev. D **70** (2004) 074030 [hep-ph/0404050].
 - [68] H. n. Li, Y. L. Shen, and Y. M. Wang, Resummation of rapidity logarithms in B meson wave functions, JHEP **02** (2013) 008 [arXiv: 1210.2978].
 - [69] H. n. Li and Y. M. Wang, Non-dipolar Wilson links for transverse-momentum-dependent wave functions, JHEP **06** (2015) 013 [arXiv: 1410.7274].
 - [70] H. n. Li, Y. L. Shen, and Y. M. Wang, Next-to-leading-order corrections to $B \rightarrow \pi$ form factors in k_T factorization, Phys. Rev. D **85** (2012) 074004 [1201.5066].
 - [71] X. Y. Han, J. Hua, X. Ji, C. D. Lü, W. Wang, J. Xu, Q. A. Zhang and S. Zhao, A new method to access heavy meson

- lightcone distribution amplitudes from first-principle, [arXiv:2403.17492 [hep-ph]].
- [72] X. Y. Han, J. Hua, X. Ji, C. D. Lü, A. Schäfer, Y. Su, W. Wang, J. Xu, Y. Yang and J. H. Zhang, *et al.* Calculation of heavy meson light-cone distribution amplitudes from lattice QCD, [arXiv:2410.18654 [hep-lat]].
 - [73] G. Buchalla, A. J. Buras, and M. E. Lautenbacher, Weak decays beyond leading logarithms, *Rev. Mod. Phys.* **68** (1996) 1125 [hep-ph/9512380].
 - [74] B. Kundu, H. n. Li, J. Samuelsson and P. Jain, The Perturbative proton form-factor reexamined, *Eur. Phys. J. C* **8** (1999) 637 [hep-ph/9806419].
 - [75] X. Liu, Bc-meson decays into J/ψ plus a light meson in the improved perturbative QCD formalism, *Phys. Rev. D* **108** (2023) 096006 [arXiv: 2305.00713].
 - [76] H. n. Li and H. S. Liao, B meson wave function in k_T factorization, *Phys. Rev. D* **70** (2004) 074030 [hep-ph/0404050].
 - [77] Y. Uchida *et al.* [Belle], Search for $\bar{B}^0 \rightarrow \Lambda_c^+ \Lambda_c^-$ decay at Belle, *Phys. Rev. D* **77** (2008) 051101 [arXiv: 0708.1105].
 - [78] C. Q. Geng, X. N. Jin and C. W. Liu, CP asymmetries in B meson two-body baryonic decays, *Phys. Lett. B* **846** (2023) 138240 [arXiv: 2306.14280].